Geodesics of Reissner-Nordstörm Black Hole with Euler-Heisenberg Parameter

by

Tehzin Zahra

Supervised by

Prof. Dr. Ibrar Hussain

Submitted in the partial fulfillment of the
Degree of Master of Philosophy
in
Mathematics

School of Natural Sciences
National University of Sciences and Technology
H-12, Islamabad, Pakistan.

2023

THESIS ACCEPTANCE CERTIFICATE

Certified that final copy of MS thesis written by **Tehzin Zahra** (Registration No. **00000330991**), of **School of Natural Sciences** has been vetted by undersigned, found complete in all respects as per NUST statutes/regulations, is free of plagiarism, errors, and mistakes and is accepted as partial fulfillment for award of MS/M.Phil degree. It is further certified that necessary amendments as pointed out by GEC members and external examiner of the scholar have also been incorporated in the said thesis.

Signature: _____

Name of Supervisor: Dr. Ibrar Hussain

Date: 26 - 6 - 2023

Signature (HoD): _____

Date: 26/06/2023

Signature (Dean/Principal): _____

Date: 26/06/2023

FORM TH-4

National University of Sciences & Technology

MS THESIS WORK

We hereby recommend that the dissertation prepared under our supervision by: **"Tehzin Zahra"** Regn No. **00000330991** Titled: **"Geodesics of Reissner-Nordström Black Hole with Euler Heisenberg Parameter"** accepted in partial fulfillment of the requirements for the award of **MS** degree.

Examination Committee Members

1. Name: DR. MUBASHER JAMIL Signature:

2. Name: DR. ADNAN ASLAM Signature:

Supervisor's Name: DR. IBRAR HUSSAIN Signature:

A/Head of Department

26/06/2023
Date

COUNTERSINGED

Date: 26/6/2023

A/Dean/Principal

Dedication

US KY NAAM PR JO “RAHMAN O RAHIM” HY!

Acknowledgements

Aw'alan, shukar us RAB UL AALAMEEN ki zaat ka jis ny is AMAR ki anjam-dahi ki tofeeq inayat farmaye. Salaat wa salam RAHMAT UL AALAMEEN ar AHL UL BAIT ki zaat aqdas pr jo RAAH E HIDAYIT pr RAH-NOMA hain.

Dow'om, Dua-go hun apny ahl e khana, asateed ar ahbab kleay jo waseela theray is amar ki takmeel main, bilkhasoos, USTAD E MOHTRAM AGHA SYED JAWAD NAQVI, nigran DR. IBRAR HUSSAIN ar GEC rukan DR. MUBASHIR JAMIL.

Contents

List of Figures

Abstract

The trajectories of nulllike and timelike geodesics for circular motion in the vicinity of Reissner-Nordström (RN) black hole with Euler-Heisenberg (EH) parameter i.e; $\mu = 9.46691 \times 10^{-6}$ are investigated and compared with RN case. We found that radius of outer horizon is same for both cases, however, unlike the RN black hole which possesses two horizons, EH case has only one horizon. We calculated energy, angular momentum and effective potential. It was seen that effective potential is not affected by adding an extra term with new parameter. The stability of circular orbits of particles is also discussed by using the effective potential of the particles.

Chapter 1

Introduction

In the late 19th century, physicists noticed a contradiction between the laws of electromagnetism (as proposed by James Clerk Maxwell) and the laws of motion (as proposed by Isaac Newton). Specifically, the laws of electromagnetism suggested that the speed of light was constant in all reference frames, while Newton's laws implied that the speed of light would depend on the relative motion of the observer. This contradiction ultimately led to the development of Albert Einstein's theory of Special Relativity [1, 2] in 1905, which introduced the concept of spacetime and showed that the speed of light is indeed constant in all reference frames.

The theory has two fundamental postulates. First, the laws of Physics are the same in all inertial frames of reference. Second, light travels in vacuum with the same speed c in any direction in all inertial frames and not relative to the movement of the observer. Later he extended these postulates to non inertial frames as well. Newton's law of universal gravitational accurately predicts much of what we see within our solar system.

Einstein presented the General theory of Relativity in 1915 [3–5]. Unlike Newton's theory which introduced gravity as a force that acts between objects or massive bodies, Einstein envisioned gravity as a spacetime curvature due to mass and energy. This unified fabric is curved and stretched by heavy objects like planets and stars, and this curving of spacetime creates what we feel as gravity. A planet like the Earth is kept in orbit because it follows a curve in a spacetime fabric caused by the Sun's curvature in spacetime. The following assumptions underpin Einstein theory:

1. The weak equivalence principle is considered as a cornerstone of the GR. It states that the motion of a freely falling body is independent of its mass in a gravitational field. More precisely, inertial and gravitational masses of a body are equivalent. Whereas, the strong equivalence principle states that no experiment can distinguish between an accelerating and gravitational frame of reference within the small regions of spacetime.

2. The covariance principle states that field equations are generally covariant tensor equations and they remain invariant in all coordinate systems. In other words, all coordi-

nate systems are physically equivalent.

Einstein's theory has important astrophysical implications. For example, it implies the existence of black holes in space and one can explore different phenomena such as gravitational lensing, gravitational time dilation and the gravitational red shift that take place in the vicinity of black holes .
Einstein gave a set of second-order partial differential equations

$$R_{\rho\sigma} - \frac{1}{2}Rg_{\rho\sigma} = kT_{\rho\sigma}, \quad (\rho, \sigma = 0, 1, 2, 3) \tag{1.1}$$

where k is the gravitational constant, defined as

$$k = \frac{8\pi G}{c^4}, \tag{1.2}$$

known as the Einstein Field Equations (EFEs). These equations, collectively known as the stress-energy-momentum tensor $T_{\rho\sigma}$, connect the presence of mass, energy, and momentum to the curvature of spacetime. In (1.1) $R_{\rho\sigma}$ is the Ricci tensor, R is its trace called the Ricci scalar and $g_{\rho\sigma}$ is the metric tensor (all these tensors will be discussed in subsequent Sections).

In 1916 Karl Schwarzschild presented first exact solution to EFEs. Schwarzschild solution [6] represents the spacetime geometry outside a static spherical symmetric matter distribution in the empty space. Vacuum solutions, electrovacuum solutions, null dust solutions, scalar field solution [7] are some of the exact solutions EFEs. Mans Reissner and Gunnar Nordström discovered RN metric [8, 9] soon after Schwarzschild metric. The Reissner-Nordström (RN) metric is indeed a solution to the (EFEs) that describes a static, spherically symmetric, and electrically charged black hole. It is a nonvacuum solution since the source has an electric charge q and hence there is an electric field that corresponds to the gravitational field of charged, spherically symmetric body of mass M. Kerr metric, presented in 1963, is exact solution for an uncharged, rotating black hole which describes the geometry of empty spacetime around a rotating uncharged axially symmetric black hole with ellipsoidal event horizon [10]. In 1965, Ezra Newmann found Kerr-Newmann (KN) metric [11]. The KN metric is a solution of the Einstein Maxwell field equations that describe the spacetime geometry in the region surrounding a charged, rotating mass [12].

A significant aspect of black hole Physics is particle motion around them. It is possible to comprehend the geometry of spacetime close to a black hole by seeing how a particle moves around it. Particle collisions and other types of astrophysical phenomena emerge from the fact that the presence of the gravitational field makes it harder for the particles to proceed on stable orbits [13]. In this regard, different authors have discussed particle

dynamics in different black hole spacetimes. The stability of precessing elliptical orbits in the Schwarzschild field was studied by Hansen [14]. It is known that circular orbits in the Schwarzschild spacetime with radii smaller than three times the Schwarzschild radius are unstable. Authors studied massive particles in a modified Schwarzschild geometry [15]. Dadhich and Kale studied timelike and null geodesics in the RN spacetime [16]. It was discovered that at a finite radial distance a turning point is always encountered by the approaching geodesics. The limitations for escape, bound, and stable orbits are discovered and shown to be nearer the source as compared with Schwarzschild spacetime [16]. Armenti investigated the circular geodesic stability and existence criterion near the RN black hole [17]. Kurmakaev analyzed circular orbits in the Kerr spacetime [18]. The radial motion of the photons in the KN spacetime was presented by Stuchlik [19]. Stuchlik discovered that there comes a qualitative difference between the Kerr and KN metrics for the radial motion of photons only within the inner horizons and near the naked singularities [19].

From the beginning to the end of this dissertation, the system of units is used where the gravitational constant G and speed of light c are equal to 1.

1.1 Metric Tensor

Metric tensor is a bilinear map of two vectors into the real numbers which means we have established an identical expression for the inner product of two vectors V and W

$$\begin{aligned} V \cdot W &= (V^\mu \partial_\mu) \cdot (W^\mu \partial_\nu)\,, \\ &= V^\mu W^\mu \,(\partial_\mu \cdot \partial_\nu)\,, \\ &= V^\mu W^\nu g_{\mu\nu}. \end{aligned} \tag{1.3}$$

Where $\partial_\mu = \frac{\partial}{\partial x^\mu}$, and x^μ are coordinates. Hence, metric tensor is the dot product of basis vectors. Its covariant and contravariant components are

$$\begin{aligned} g_{\mu\nu} &= g(dx^\mu, dx^\nu) = dx^\mu \cdot dx^\nu, \\ g^{\mu\nu} &= g(\partial_\mu, \partial_\nu) = \partial_\mu \cdot \partial_\nu. \end{aligned} \tag{1.4}$$

Metric can be viewed as the line element which gives the distance between two points $x^\mu(\lambda_0)$ and $x^\mu(\lambda_0 + \Delta\lambda_0)$ on a world-line $x^\mu(\lambda)$ of a particle. Let V^α denote the tangent vector field to the curve,

$$ds^2 = g(V,V)d\Omega^2 = g_{\alpha\beta}V^\alpha V^\beta d\Omega^2 = g_{\alpha\beta}dx^\alpha dx^\beta. \tag{1.5}$$

Here $V^\alpha = \frac{dx^\alpha}{d\Omega}$. It is usually non-degenerate, $g = \det(g_{\alpha\beta}) \neq 0$. Inverse of the metric $g_{\mu\nu}$ exists and unique, i.e

$$g_{\sigma\lambda}g^{\lambda\mu} = g^{\mu\nu}g_{\nu\sigma} = \delta^\mu{}_\sigma; \qquad \mu,\nu,\sigma,\lambda = 0,1,2,3. \tag{1.6}$$

1.2 Covariant Derivative

Covariant derivative is a more advanced rule of differentiation as partial derivatives do not keep the fundamental properties, for instance transformation law, of a tensor. The mathematical expression of covariant derivative of a covector is

$$X_{\mu;\nu} = X_{\mu,\nu} - \Gamma^{\eta}_{\mu\nu} X_{\eta}, \tag{1.7}$$

where Γ denotes the christoffel symbol given as

$$\Gamma^{\alpha}_{\beta\nu} = \frac{1}{2} g^{\alpha\eta} \bigg(g_{\eta\beta,\nu} + g_{\eta\nu,\beta} - g_{\beta\nu,\eta} \bigg). \tag{1.8}$$

For a contravariant vector

$$X^{\mu}_{;\nu} = X^{\mu}_{,\nu} + \Gamma^{\mu}_{\eta\nu} X^{\eta}. \tag{1.9}$$

For mixed tensor

$$X^{\mu}_{\gamma;\nu} = X^{\mu}_{\gamma,\nu} + \Gamma^{\mu}_{\alpha\nu} X^{\alpha}_{\gamma} - \Gamma^{\beta}_{\gamma\nu} X^{\mu}_{\beta}. \tag{1.10}$$

1.3 Geodesics

A geodesic is the shortest path between two points on a curved surface, such as a straight line on a sphere or curved spacetime. Geodesic is a curve along which the tangent vector is transported parallelly as it moves along the curve. In other words, the direction of the tangent vector remains constant along the geodesic. Let $x^{\mu}(\lambda)$ be the worldline or path and $\frac{dx^{\mu}}{d\lambda}$ be the tangent vector field to $x^{\mu}(\lambda)$.The tangent vector field is parallel transported to the curve if the following condition is satisfied [20]

$$\frac{d^2 x^{\mu}}{d\lambda^2} + \Gamma^{\mu}_{\nu\rho} \frac{dx^{\nu}}{d\lambda} \frac{dx^{\rho}}{d\lambda} = 0. \tag{1.11}$$

In flat spacetime, freely falling particles move along straight lines. Mathematically, it can be expressed as the second derivative of the parametrized path $x^{\mu}(\lambda)$ becomes zero

$$a^{\mu} \equiv \frac{d^2 x^{\mu}}{d\lambda^2} = 0. \tag{1.12}$$

This is not a tensorial form. Its tensorial form is written as

$$\frac{d^2 x^{\mu}}{d\lambda^2} = V^{\alpha} \partial_{\alpha} V^{\mu} = 0. \tag{1.13}$$

Now by replacing partial derivative with a covariant derivative to get a generalized form for curved space

$$V^{\alpha} V^{\mu}{}_{;\alpha} = 0. \tag{1.14}$$

Hence, the motion of the free particles can be described through geodesics.

1.4 The Einstein Field Equations with Energy and Matter

EFEs give a relation between the spacetime curvature and matter distribution within it. Einstein tensor contains the information about curvature of spacetime while stress-energy tensor is related with mass density, energy density, pressure and other physical properties. EFEs are derived using the Lagrangian formalism. Let $\mathcal{S}_g$ denotes the gravitational action integral and $\mathcal{S}_m$ be the energy-matter action integral. The variation of the action by considering a local inertial frame is given by

$$\delta\mathcal{S} = \delta\big(\mathcal{S}_m + \mathcal{S}_g\big), \tag{1.15}$$

here

$$\mathcal{S}_g = \frac{1}{2k}\int_{\nu}\sqrt{-g}Rd^4x, \quad \mathcal{S}_m = \frac{1}{2k}\int_{\nu}L_m\sqrt{-g}d^4x. \tag{1.16}$$

Here $k = 8\pi$ and is obtained when we take EFEs in the weak field limit. L_m denotes the Lagrangian and is a function of x^α and $\dot{x}^\alpha$ explaining the dynamics of the physical system [21]. Consider an infinitesimally small region ν in which variation of the action $\mathcal{S}$ takes place with some restrictions to the variation at the boundary i.e., $\delta g_{\mu\nu}|_{\partial\nu} = 0$ and $\delta g_{\mu\nu,\lambda}|_{\partial\nu} = 0$. First we calculate $\delta\mathcal{S}_g$ and then $\delta\mathcal{S}_m$,

$$\begin{aligned}\delta\mathcal{S}_g &= \frac{1}{2k}\int_{\nu}\delta\Big[R_{\alpha\beta}g^{\alpha\beta}\sqrt{-g}\Big]d^4x,\\ &= \frac{1}{k}\int_{\nu}\Big[g^{\alpha\beta}\sqrt{-g}\delta R_{\alpha\beta} + R_{\alpha\beta}\delta\Big(g^{\alpha\beta}\sqrt{-g}\Big)\Big]d^4x.\end{aligned} \tag{1.17}$$

Since we consider a local inertial frame which means $\Gamma^\eta_{\alpha\beta} = 0$ and $\Gamma^\eta_{\alpha\beta,\lambda} \neq 0$ therefore

$$R_{\alpha\beta} = \Gamma^\eta_{\alpha\beta,\eta} - \Gamma^\eta_{\alpha\eta,\beta}. \tag{1.18}$$

Apply the variation on (1.18), we get

$$\delta R_{\alpha\beta} = \delta\Gamma^\eta_{\alpha\beta,\eta} - \delta\Gamma^\eta_{\alpha\eta,\beta}. \tag{1.19}$$

Since $\Gamma^\eta_{\alpha\beta}$ is not a tensor, so ∂_μ can be replaced by ∇_α

$$g^{\alpha\beta}\delta R_{\alpha\beta} = g^{\alpha\beta}\big(\delta\Gamma^\eta_{\alpha\beta}\big)_{;\eta} - g^{\alpha\beta}\big(\delta\Gamma^\eta_{\alpha\eta}\big)_{;\beta}. \tag{1.20}$$

Now interchange the indices of the second term of the right-hand side as $\beta \longrightarrow \eta$, (1.20) yields

$$g^{\mu\nu}\delta R_{\mu\nu}\big(g^{\mu\nu}\delta\Gamma^\eta_{\mu\nu} - g^{\mu\eta}\delta\Gamma^\nu_{\mu\nu}\big)_{;\eta}, \tag{1.21}$$

where $g^{\mu\nu}{}_{;\eta} = 0$. Consider a vector

$$N^\eta = g^{\mu\nu}\delta\Gamma^\eta_{\mu\nu} - g^{\mu\eta}\delta\Gamma^\nu_{\mu\nu}. \tag{1.22}$$

Using (1.22) in (1.21) we get

$$g^{\mu\nu}\delta R_{\mu\nu} = N^{\eta}_{;\eta}, \tag{1.23}$$

$$\int_{\nu} \sqrt{-g} g^{\mu\nu}\delta R_{\mu\nu} d^4x = \int_{\nu} \sqrt{-g} N^{\eta}_{;\eta} d^4x. \tag{1.24}$$

By using the *Gauss Divergence theorem*, which establishes a relationship between the volume integral of the divergence of a vector field and its surface boundary integral as

$$\int_{\nu} \sqrt{-g} N^{\eta}_{;\eta} d^4x = \int_{\partial\nu} u_{\eta} N^{\eta} \sqrt{-g} d^3y, \tag{1.25}$$

where $N^{\eta}_{;\eta}$ denotes the divergence of N^{η} and u_{η} implies the unit normal to the surface [22], so the left-hand side of (1.24) vanishes

$$\int_{\nu} \sqrt{-g} g^{\mu\nu}\delta R_{\mu\nu} d^4x = 0. \tag{1.26}$$

Also

$$\delta\big(g^{\alpha\beta}\sqrt{-g}\big) = \sqrt{-g}\delta g^{\alpha\beta} - g^{\alpha\beta}\big(\frac{1}{2}\sqrt{-g} g_{\mu\nu}\delta g^{\mu\nu}\big). \tag{1.27}$$

Putting the values of (1.27) and (1.28) in (1.17) one obtains

$$\delta\mathcal{S}_g = \frac{1}{2k}\int_{\nu}\left[\sqrt{-g}R_{\alpha\beta}\Big(\delta g^{\alpha\beta} - \frac{1}{2}g^{\alpha\beta}g_{\mu\nu}\delta g^{\mu\nu}\Big)\right] d^4x. \tag{1.28}$$

Now we calculate $\delta\mathcal{S}_m$

$$\begin{aligned} \delta\mathcal{S}_m &= \int_{\nu}\delta\Big(L_m\sqrt{-g}\Big)d^4x, \\ &= \int_{\nu}\left[L_m\delta\Big(\sqrt{-g}\Big) + \sqrt{-g}\delta\Big(L_m\Big)\right]d^4x. \end{aligned} \tag{1.29}$$

Using $\delta g = -g g_{\alpha\beta}\delta g^{\alpha\beta} = g g^{\alpha\beta}\delta g_{\alpha\beta}$ and $\delta\sqrt{-g} = -\frac{1}{2}\big(\sqrt{-g}g_{\alpha\beta}\delta g^{\alpha\beta}\big)$, (1.29) becomes

$$\delta\mathcal{S}_m = -\frac{1}{2}\int_{\nu}\left[g_{\alpha\beta}L_m - 2\frac{\delta L_m}{\delta g^{\alpha\beta}}\right]\sqrt{-g}\delta g^{\alpha\beta}d^4x. \tag{1.30}$$

Now flux and density of energy and momentum are described by energy-momentum tensor defined as

$$T_{\alpha\beta} = g_{\alpha\beta}L_m - 2\frac{\delta L_m}{\delta g^{\alpha\beta}}. \tag{1.31}$$

Using (1.28),(1.30), and (1.31), (1.15) attains the form

$$\begin{aligned} \delta\mathcal{S} &= \frac{1}{2k}\int_{\nu}\sqrt{-g}R_{\alpha\beta}\Big(\delta g^{\alpha\beta} - \frac{1}{2}g^{\alpha\beta}g_{\mu\nu}\delta g^{\mu\nu}\Big)d^4x - \frac{1}{2}\int_{\nu}\sqrt{-g}T_{\alpha\beta}\delta g^{\alpha\beta}d^4x, \\ \delta\mathcal{S} &= \frac{1}{2k}\int_{\nu}\sqrt{-g}\Big(R_{\alpha\beta} - \frac{1}{2}Rg_{\alpha\beta} - kT_{\alpha\beta}\Big)\delta g^{\alpha\beta}d^4x. \end{aligned} \tag{1.32}$$

As $\delta\mathcal{S} = 0$, for an arbitrary variation we have $\delta g^{\alpha\beta} \neq 0$, and we get EFEs

$$R_{\alpha\beta} - \frac{1}{2}Rg_{\alpha\beta} = kT_{\alpha\beta}, \tag{1.33}$$

where $R_{\alpha\beta} - \frac{1}{2}Rg_{\alpha\beta} \equiv G_{\alpha\beta}$, is known as *Einstein tensor* which is a second rank symmetric tensor.

1.5 Riemann Curvature Tensor and its Properties

In GR, the curvature of spacetime indicated that gravity is present. This curvature is measured by the curvature tensor, also known as the Reimann tensor [23]. Reimann tensor is defined as:

$$R^{\sigma}_{\alpha\beta\lambda} = \Gamma^{\sigma}_{\alpha\lambda,\beta} - \Gamma^{\sigma}_{\alpha\beta,\lambda} + \Gamma^{\sigma}_{\eta\beta}\Gamma^{\eta}_{\alpha\lambda} - \Gamma^{\sigma}_{\eta\lambda}\Gamma^{\eta}_{\alpha\beta}. \tag{1.34}$$

In Riemannian geometry, curvature invariants are scalar quantities and usually obtained by using the Reimann tensor which describes the curvature of spacetime, given by

$$\begin{aligned} I_1 &= R, \\ I_2 &= R^{\alpha\beta}R_{\alpha\beta}, \\ I_3 &= R^{\alpha\beta\sigma\rho}R_{\alpha\beta\sigma\rho}. \end{aligned} \tag{1.35}$$

In (1.35) I_1 is the first, I_2 is second and I_3 is the third curvature invariant, R and $R_{\mu\nu}$ denote Ricci scalar and Ricci tensor which are defined as

$$\begin{aligned} R = R^{\alpha}_{\alpha} &= g^{\alpha\beta}R_{\alpha\beta}, \\ R_{\alpha\beta} &= g^{\lambda\sigma}R_{\lambda\alpha\sigma\beta} = R^{\sigma}_{\alpha\sigma\beta}. \end{aligned} \tag{1.36}$$

$R^{\lambda}{}_{\beta\mu\nu}$ can also be written as

$$R_{\alpha\beta\mu\nu} = g_{\alpha\lambda}R^{\lambda}{}_{\beta\mu\nu}. \tag{1.37}$$

The Riemann tensor has n^4 independent components, where n represents dimensions. It is anti-symmetric with respect to the first two and last two indices leading to the following symmetries

$$R_{\alpha\beta\rho\sigma} = -R_{\beta\alpha\rho\sigma} = -R_{\alpha\beta\sigma\rho} = R_{\rho\sigma\alpha\beta}. \tag{1.38}$$

The Riemann tensor satisfies the below mentioned *Bianchi identities* as

$$R^{\alpha}_{\beta\rho\sigma} + R^{\alpha}_{\sigma\beta\rho} + R^{\alpha}_{\rho\sigma\beta} = 0, \tag{1.39}$$

$$R_{\alpha\beta\rho\sigma;\lambda} + R_{\alpha\beta\lambda\rho;\sigma} + R_{\alpha\beta\sigma\lambda;\rho} = 0. \tag{1.40}$$

The difference (1.38) - (1.39) yields $R^{\alpha}_{\beta\rho\sigma} = 0$, and the number of independent components is $\frac{n^2}{12}\big(n^2 - 1\big)$.

1.6 Stress-Energy-Momentum Tensor

As mentioned before, the stress-energy-momentum tensor is source term of EFEs. It describes the distribution of matter and energy within a curved spacetime along with the physical properties, for instance, mass density, energy density, flux of energy and momentum and pressure of material things. The component T^{00} represents the energy density while, $T^{0\beta}$ (T^{01}, T^{02} and T^{03}) indicate energy flux in the β-direction . $T^{\alpha 0}$ (T^{10}, T^{20} and T^{30}) are the momentum densities. $T^{\alpha\beta}$ is the rate of flow of the α-component of momentum per unit area in the β-direction [12].

For example, for a perfect fluid there exist no opposing forces between the particles to let them keep moving, no viscosity or heat conduction in the instantaneous rest frame and mathematically expressed as

$$T^{\alpha\beta} = \Big(\rho + \frac{p}{c^2}\Big)V^{\alpha}V^{\beta} + pg^{\alpha\beta}, \tag{1.41}$$

here ρ, p, V^{α} are the density, pressure and four-velocity of the fluid respectively. Dust (pressureless fluid) is a special case for perfect fluid. Its mathematical expression is mentioned below:

$$T^{\alpha\beta} = \rho V^{\alpha}V^{\beta} \quad \big(p = 0\big).$$

The energy-momentum tensor for an electromagnetic field is

$$T^{\alpha\beta}_{(em)} = \frac{-1}{a_0}\Big[F^{\alpha}_{\sigma}F^{\beta\sigma} - \frac{1}{4}g^{\alpha\beta}F_{\sigma\rho}F^{\sigma\rho}\Big], \tag{1.42}$$

where a_0 is the constant and $F^{\alpha\beta}$ denotes the Maxwell or electromagnetic tensor.

1.7 Effective Potential

In classical mechanics, the motion of a particle is given through the following equation[1]

$$\frac{1}{2}\Big(\frac{dr}{dt}\Big)^2 + V_{eff}(r) = E, \tag{1.43}$$

where $V_{eff}(r)$ indicates the effective potential and E denotes the total energy of the particle per unit mass. The effective potential of an orbiting body around a spherical mass M is given as

$$V_{eff}(r) = \frac{L^2}{2r^2} - \frac{M}{r}. \tag{1.44}$$

where L is the angular momentum of the particle per unit mass. E and L are also known as the total energy and angular momentum of the particle, respectively.

[1] (1.43) comes from E = Total energy = Kinetic energy + Potential energy = $\frac{1}{2}m(\dot{r}^2 + r^2\dot{\phi}^2) - \frac{Mm}{r}$, where $\dot{\phi} = \frac{L}{r^2}$.

1.8 Black Holes

Massive stars are primarily composed of gases such as hydrogen and helium along with dust clouds. When a star exhausts its nuclear fuel and balance between the internal pressure and gravitational pull is disrupted. At this stage, the star undergoes collapsed due to its own gravity. The entire matter shrinks to a point called *Singularity* [24].
The final state of the collapse depends on the size of the star, leading to three possible types,
(1) White Dwarf: A white dwarf is the final state of a star with a relatively low mass and they are nearly the size of the Earth. The critical mass limit for a star to become a white dwarf is $M \leq 1.44 M_{\odot}$[2] known as Chandrasekhar limit. A white dwarf is supported by the electron degeneracy pressure.
(2) Neutron Star: If the star has mass such that $1.4 M_{\odot} \leq M \leq 3.2 M_{\odot}$, then the gravitational collapse overcomes the neutron degeneracy pressure. In this case, the star becomes a neutron star, which is extremely dense and composed mainly of neutrons.
(3) Black Hole: Stars with a mass greater than approximately three times the mass of the Sun ($3 M_{\odot}$) continue to collapse further. The gravitational forces become so strong that even light cannot escape. These collapsed stars become black holes, characterized by their intense gravitational pull. Black holes are usually found at the center of galaxies. The region of spacetime where the gravitational effects are so strong that nothing can escape from inside it, neither particles nor light is known as *Event Horizon*.

There are two types of singularities,
(1) Coordinate singularity
(2) Naked singularity

These singularities can be defined through the curvature invariants I_1, I_2 and I_3 (specified in (1.35)). A coordinate singularity cannot be considered a physical singularity and can be removed by using different other coordinates, for example, Eddington-Finkelstein and Kruskal coordinate etc. The above-mentioned invariants must be finite at a singular point to be a coordinate singularity. However, naked singularity is physical singularity and cannot be removed by using any other coordinate system and I_1, I_2 and I_3 do not possess a finite value.

R. Ruffini and J.A. Wheeler invented the term black hole in 1967 [25]. The black hole is a spacetime region whose specialty is being disconnected from the rest of space. Mathematically it is expressed by a metric or line element and it is singular solution to the EFEs. The below-mentioned black holes are few examples of different black holes.

[2] $M_{\odot}$ is the solar mass i.e. $1.9891 \times 10^{30} kg$.

1.8.1 Schwarzschild Solution

The first exact solution to the EFEs is given by

$$ds^2 = -\Big(1 - \frac{2M}{r}\Big)dt^2 + \Big(1 - \frac{2M}{r}\Big)^{-1}dr^2 + r^2\Big(d\theta^2 + \sin^2\theta d\phi^2\Big), \tag{1.45}$$

where r is the radial coordinate and M is the mass of the central object. The event horizon can be obtained as

$$1 - \frac{2M}{r} = 0, \qquad \Rightarrow \quad r_h = 2M. \tag{1.46}$$

There are two singularities for metric (1.45) at $r_h = 2M$ and $r = 0$. The curvature invariants indicate that $r = 0$ is a naked singularity but at $r_h = 2M$ the singularity is removable by using a different system of coordinates. Invariants are given as:

$$\begin{aligned} I_1 &= 0, \\ I_2 &= 0, \end{aligned} \tag{1.47}$$

$$I_3 = \frac{48M^2}{r^6}. \tag{1.48}$$

1.8.2 Reissner-Nordström Solution

The metric is given by

$$ds^2 = -\Big(1 - \frac{2M}{r} + \frac{Q^2}{r^2}\Big)dt^2 + \Big(1 - \frac{2M}{r} + \frac{Q^2}{r^2}\Big)^{-1}dr^2 + r^2\Big(d\theta^2 + \sin^2\theta d\phi^2\Big), \tag{1.49}$$

here M and Q denote mass and total electric charge on a black hole. The horizon radii are given as

$$r_\pm = M \pm \sqrt{M^2 - Q^2}.$$

When $Q = 0$, r_+ reduces to Schwarzschild's horizon and hence is an event horizon.
The curvature invariants are:

$$\begin{aligned} I_1 &= 0, \\ I_2 &= \frac{4Q^4}{r^8}. \end{aligned} \tag{1.50}$$

We can notice that $r = 0$ is a coordinate singularity.

Chapter 2

Schwarzschild Geodesics with String Cloud Parameter

This chapter is devoted to a comprehensive review of the "Schwarzschild Geodesics with String Cloud Parameter" [26]. The main focus of this chapter is to examine and analyze the effect of the string cloud parameter α on the trajectories of timelike and null geodesics. These trajectories are then compared to the standard Schwarzschild geodesics, allowing for a detailed investigation into the impact of the string cloud parameter on the behavior of particles moving in the curved spacetime described by the Schwarzschild metric.

Strings are axially symmetric, cylindrical, and line-like formations which are topological defects brought on by the symmetry breaking of the field. The collection of strings is referred to as "string cloud". Cosmic strings intersect with each other during the expansion of the universe and may cause density perturbations that eventually cause galaxy formation. Strings can be detected through gravitational lensing and gravitational waves.

String cloud model was proposed by Letelier [27]. Sharif and Iftikhar studied null geodesics and strong gravitational lensing in a string cloud background [28]. In [26] trajectories of the timelike and null geodesics with string cloud parameter were studied. It was examined that if α becomes zero the result reduces to Schwarzschild case.

We have structured this chapter in the following manner. Section 2.1 provides a comprehensive overview of the particle trajectories and effective potential in the context of Schwarzschild spacetime with string cloud parameter. This section serves as a review, setting the foundation for the subsequent discussions. Section 2.2 delves into the trajectories of the timelike and null geodesics for circular motion for Schwarzschild spacetime with string cloud parameter. Additionally, we include plots to visually depict these trajectories, aiding in the understanding of their behavior and characteristics.
The action of the string evolving in the spacetime is

$$S = \int M_0 \sqrt{-\det(\gamma_{ab})} d\lambda^0 d\lambda^1, \tag{2.1}$$

where M_0 is a positive constant that specifies each string and

$$\gamma_{ab} = g_{\alpha\beta}\frac{\partial x^\alpha}{\partial \lambda^a}\frac{\partial x^\beta}{\partial \lambda^b} \quad a, b = 0, 1 \tag{2.2}$$

(2.2) represents two dimensional world sheet as String moves in two dimensions and creates a world sheet in spacetime. $x^\alpha = x^\alpha(\lambda^a)$ is the world sheet with parameters λ^0 for timelike and λ^1 for spacelike. The energy-momentum tensor for a string cloud is

$$T^{\alpha\beta} = \rho_0(\xi^{\alpha\sigma}\xi_\sigma{}^\beta)(-\gamma)^{-\frac{1}{2}}, \tag{2.3}$$

where a bivector $\xi^{\alpha\beta}$ is an antisymmetric tensor of second rank, defined as [27]

$$\xi^{\alpha\beta} = \epsilon^{ab}\frac{\partial x^\alpha}{\partial \lambda^a}\frac{\partial x^\beta}{\partial \lambda^b}, \tag{2.4}$$

here ϵ^{ab} is the two dimensional Levi Civita symbol normalized as: $\epsilon^{01} = -\epsilon^{10} = 1$.
We would solve EFEs to get the general solution for string cloud in spherical symmetry in mixed form. The general static spherically symmetric metric is,

$$ds^2 = -e^{\nu(r)}dt^2 + e^{\lambda(r)}dr^2 + r^2\sin^2\theta d\phi^2, \tag{2.5}$$

here ν and λ are functions of r. Using $T^{\mu\nu}$, Ricci scalar and Ricci tensor in the EFEs for the clouds [26]

$$\nu = -\lambda, \tag{2.6}$$

$$e^{-\lambda} = 1 - \alpha + \frac{\beta}{r}, \tag{2.7}$$

where β is the constant of integration. By considering the weak field limit we can identify β as

$$\beta = -2M. \tag{2.8}$$

Where M is mass of a gravitational source which is spherically symmetric. Hence the spacetime metric is

$$ds^2 = -\Big(1 - \frac{2M}{r} - \alpha\Big)dt^2 + \Big(1 - \frac{2M}{r} - \alpha\Big)^{-1}dr^2 + r^2\Big(d\theta^2 + \sin^2\theta d\phi^2\Big). \tag{2.9}$$

The above metric represents the spacetime geometry around a black hole with mass M encircled by a spherical cloud of strings. Here α is "string cloud parameter". For the realistic model string cloud parameter is restricted to $0 < \alpha < 1$.

The horizon of (2.9) is given by

$$1 - \frac{2M}{r} - \alpha = 0$$

$$r_h = \frac{2M}{1-\alpha}, \quad \alpha \in (0, 1).$$

2.1 Particle Trajectories

The Lagrangian for the geodesics of the particle in the spacetime described by (2.9) is given as

$$\mathcal{L} = \frac{m}{2} g_{\mu\nu} \dot{x}^\mu \dot{x}^\nu = m\Big(-\frac{1}{2} f(r)\dot{t}^2 + \frac{\dot{r}^2}{2f(r)} + \frac{1}{2} r^2 \Big(\dot{\theta}^2 + \sin^2\theta \dot{\phi}^2\Big)\Big). \tag{2.10}$$

Throughout this dissertation dot represents the derivative with respect to the geodetic parameter λ. The Euler-Lagrange (EL) equations are

$$\frac{d}{d\lambda}\Big(\frac{\partial \mathcal{L}}{\partial \dot{x}^\eta}\Big) = \frac{\partial \mathcal{L}}{\partial x^\eta}, \quad (\eta = 0, 1, 2, 3) \tag{2.11}$$

For $\eta = 0$, (2.11) gives,

$$\begin{aligned} &\frac{d}{d\lambda}\Big(\frac{\partial \mathcal{L}}{\partial \dot{t}}\Big) = 0, \quad \text{as} \quad \frac{\partial \mathcal{L}}{\partial t} = 0 \\ &\frac{d}{d\lambda}\Big(\frac{\partial \mathcal{L}}{\partial \dot{t}}\Big) = \frac{d}{d\lambda}\Big(- f(r)\dot{t}\Big) = 0. \end{aligned} \tag{2.12}$$

Integrating with respect to λ, we obtain

$$-f(r)\dot{t} = \text{constant} = \frac{e}{m} = E, \tag{2.13}$$

where E is the integration constant. Since we have static spherically symmetric spacetime and invariance under time translation, this leads to conservation of energy, hence the conserved quantity for the particle is the energy per unit mass. The last equation can be arranged as

$$\dot{t} = \frac{e}{f(r)m} = \frac{-E}{f(r)}, \tag{2.14}$$

where

$$f(r) = \Big(1 - \frac{2M}{r} - \alpha\Big)$$

For $\eta = 3$, we get

$$\frac{d}{d\lambda}\Big(\frac{\partial \mathcal{L}}{\partial \dot{\phi}}\Big) = \frac{\partial \mathcal{L}}{\partial \phi},$$

which implies

$$\dot{\phi} r^2 \sin^2\theta = \text{constant} = \frac{l}{m} = L, \tag{2.15}$$

where L is the integration constant. We have static spherical symmetric spacetime and invariance under spatial rotation leads to the fact that the angular momentum is conserved, so here the conserved quantity is the magnitude of the angular momentum. The direction of the angular momentum is conserved means that the particle is moving in a plane. Consider the equatorial plane of our coordinate system. In the equatorial plane, consider $\theta = \frac{\pi}{2}$.

(2.15) becomes $L = r^2\dot{\phi}$.
The normalization condition for four-velocity as

$$g_{\mu\nu}\frac{dx^\mu}{d\lambda}\frac{dx^\nu}{d\lambda} = -\epsilon. \tag{2.16}$$

Where $\epsilon = 1$, $\epsilon = -1$, and $\epsilon = 0$, for timelike, spacelike and null geodesics respectively.
In the equatorial plane, $\theta = \frac{\pi}{2}$, (2.16) implies

$$-f(r)\dot{t}^2 + \frac{\dot{r}^2}{f(r)} + r^2\dot{\phi}^2 = -\epsilon, \tag{2.17}$$

substituting $\dot{t}$ and $\dot{\phi}$ in above equation yields

$$\left(\frac{dr}{d\lambda}\right)^2 = E^2 - f\,(r)\left(\epsilon + \frac{L^2}{r^2}\right), \tag{2.18}$$

$$\frac{1}{2}\left(\frac{dr}{d\lambda}\right)^2 + V_{eff}(r) = \frac{1}{2}E^2, \tag{2.19}$$

here $V_{eff}(r) = \frac{1}{2}\left(1 - \frac{2M}{r} - \alpha\right)\left(\epsilon + \frac{L^2}{r^2}\right)$, is the effective potential. The corresponding effective energy is

$$E_{eff} = \frac{1}{2}E^2. \tag{2.20}$$

If we compare the effective potential with Schwarzschild case, it is concluded that effective potential is decreasing as the value of string cloud parameter is increasing.

2.2 Circular Motion

In the current section, the circular motion of massless and massive particles is studied. For circular motion we have r = constant, and hence $\dot{r} = \ddot{r} = 0$. For convenience, $r = \frac{1}{u}$ is introduced. Consider $\frac{du}{d\phi} = 0$ at $u = u_c$ where $r_c = \frac{1}{u_c}$ represents the radius of the circular orbit of the particle.
Consider the chain rule,

$$\dot{r} = \frac{dr}{d\xi} = \frac{dr}{d\phi}\frac{d\phi}{d\xi} = \frac{dr}{d\phi}\frac{L}{r^2}, \tag{2.21}$$

(2.18) becomes

$$\left(\frac{du}{d\phi}\right)^2 = \frac{E^2}{L^2} - \left(1 - 2Mu - \alpha\right)\left(\frac{\epsilon}{L^2} + u^2\right), \tag{2.22}$$

$$\left(\frac{du}{d\phi}\right)^2 = \frac{E^2}{L^2} - u^2 + 2Mu^3 - \frac{\epsilon}{L^2} + \frac{2M\epsilon}{L^2}u + \frac{\alpha\epsilon}{L^2} + \alpha u^2. \tag{2.23}$$

Differentiating (2.23) w.r.t ϕ

$$\frac{d^2u}{d\phi^2} = -u + 3Mu^2 + \frac{M\epsilon}{L^2} + \alpha u, \tag{2.24}$$

if $u = u_c$

$$\frac{E^2}{L^2} - \Big(\frac{\epsilon}{L^2} + u_c^2\Big)\Big(1 - 2Mu_c - \alpha\Big) = 0. \tag{2.25}$$

In the circular motion we have $\dfrac{d^2u}{d\phi^2} = 0$, therefore for (2.25) we have

$$\frac{d}{du}\left[\frac{E^2}{L^2} - \left(1 - 2Mu + \frac{2\alpha}{u}\right)\Big(\frac{\epsilon}{L^2} + u^2\Big)\right]_{u=u_c} = 0. \tag{2.26}$$

Above conditions leads to the angular momentum as

$$3Mu_c^2 + \frac{M\epsilon}{L^2} + \alpha u_c - u_c = 0, \tag{2.27}$$

solving for L^2 gives

$$L^2 = \frac{M\epsilon}{u_c\big(1 - \alpha - 3Mu_c\big)}. \tag{2.28}$$

Energy of the particle: Substituting (2.28) in (2.25)

$$\frac{E^2}{L^2} - \epsilon\left(\frac{u_c\big(1 - \alpha - 3Mu_c\big)}{M\epsilon}\right) - u_c^2 + 2M\epsilon u_c\left(\frac{\big(1 - \alpha - 3Mu_c\big)}{M\epsilon}\right), \tag{2.29}$$

solving for E^2 gives,

$$E^2 = \frac{\epsilon\big(\alpha + 2Mu_c - 1\big)^2}{\big(1 - \alpha - 3Mu_c\big)}. \tag{2.30}$$

Energy must be positive for acceptable motion of the particle, which means $1 - \alpha - 3Mu_c$ must be greater than zero. Hence $1 - \alpha - 3Mu_c > 0$, gives

$$r_c > \frac{3M}{1 - \alpha} = r_{c_{min}}. \tag{2.31}$$

Where $r_{c_{min}}$ is minimum radius of the circular orbit. Since the horizon is

$$r_h = \frac{2M}{1 - \alpha}. \quad \alpha \in (0, 1) \tag{2.32}$$

Here minimm radius of the circular orbit is larger than the horizon. Hence, a particle is unable to set a circular orbit with $r < \frac{3M}{1-\alpha}$, around a spherical massive body as the geodesic equation $r^2\dot{\phi} = L$ cannot be satisfied for circular orbits with $r < \frac{3M}{1-\alpha}$.

2.2.1 Null Geodesics

Since, for the massless particles minimum radius for circular photon orbit is

$$\alpha r_c - r_c + 3M = 0, \tag{2.33}$$

which gives

$$r_c = \frac{3M}{1-\alpha}. \tag{2.34}$$

For null case (2.25) yields

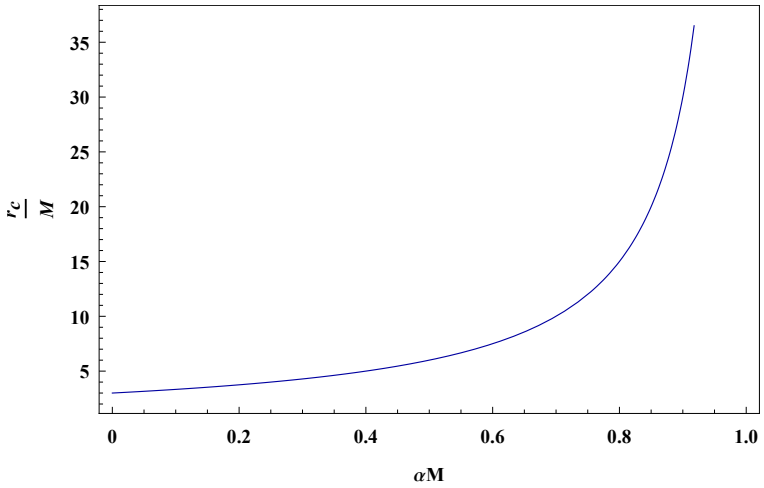

Figure 2.1: The plot of $\frac{r_c}{M}$ against αM shows the radius of the circular orbit of photon is increasing for larger value of α.

$$\frac{E^2}{L^2} = \left(1 - 2Mu_c - \alpha\right)\left(u_c^2\right), \tag{2.35}$$

$$\frac{E^2}{L^2} = \left(\frac{1-\alpha}{3M}\right)^2 - 2M\left(\frac{1-\alpha}{3M}\right)^3 - \alpha\left(\frac{1-\alpha}{3M}\right)^2, \tag{2.36}$$

after simplification

$$\frac{E^2}{L^2} = \frac{\left(1-\alpha\right)^3}{27M^2}. \tag{2.37}$$

If the values of r_c, M and α are known, it means there exists only one equilibrium circular orbit for photon with the ratio $\frac{E^2}{L^2}$.

Stability: Consider the geodesic equation (2.18) and a substitution of $\tau = \frac{\tilde{\tau}}{L}$, implies

$$\left(\frac{dr}{d\tilde{\tau}}\right)^2 + V_{eff}(r) = E_{eff}(r), \tag{2.38}$$

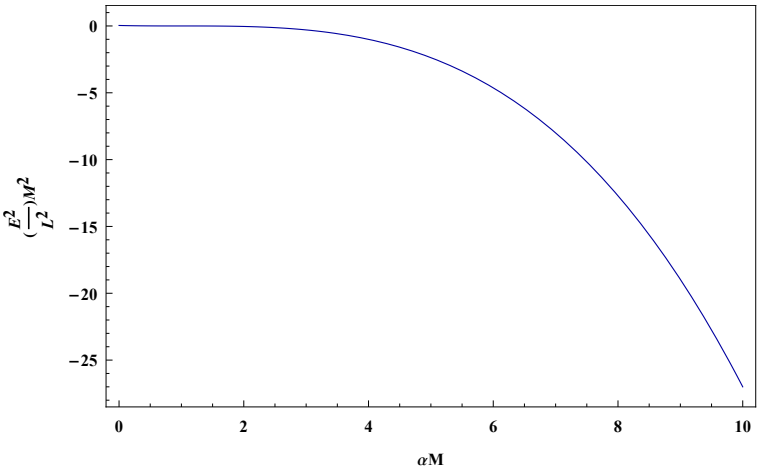

Figure 2.2: The plot of $(\frac{E^2}{L^2})M^2$ against string cloud parameter for photon. The circular orbit of photon has decreasing value of $(\frac{E^2}{L^2})$ as the value of α is increasing.

here

$$V_{eff}(r) = \frac{\left(1 - \frac{2M}{r} - \alpha\right)}{r^2} = \frac{1}{r^2} - \frac{2M}{r^3} - \frac{\alpha}{r^2}. \tag{2.39}$$

$$E_{eff}(r) = \frac{E^2}{L^2}. \tag{2.40}$$

A circular orbit becomes stable if $\frac{dV_{eff}}{dr} = 0$, and $\frac{d^2V_{eff}}{dr^2} > 0$, at r_c

$$V''_{eff}(r) = (6 - 6\alpha)\left(\frac{1-\alpha}{3M}\right)^4 - 24M\left(\frac{1-\alpha}{3M}\right)^5. \tag{2.41}$$

V''_{eff} is negative for different values of α ranges between $(0, 1)$ hence, photons possess no stable circular orbit.

Circular orbits can be stable or unstable. If the circular orbit corresponds to the minimum of the effective potential, it is stable. In this case, any perturbation of the orbit will result in small oscillation around the equilibrium position of the orbit. On the other hand, if the circular orbit corresponds to the maximum of the potential then it is unstable. In this case, any perturbation will result in the particle to move away from its equilibrium position either to infinity or drop into singularity. We have plotted V_{eff} in figure 2.3 showing there exists no stable circular orbit for different values of string cloud parameters for photons.

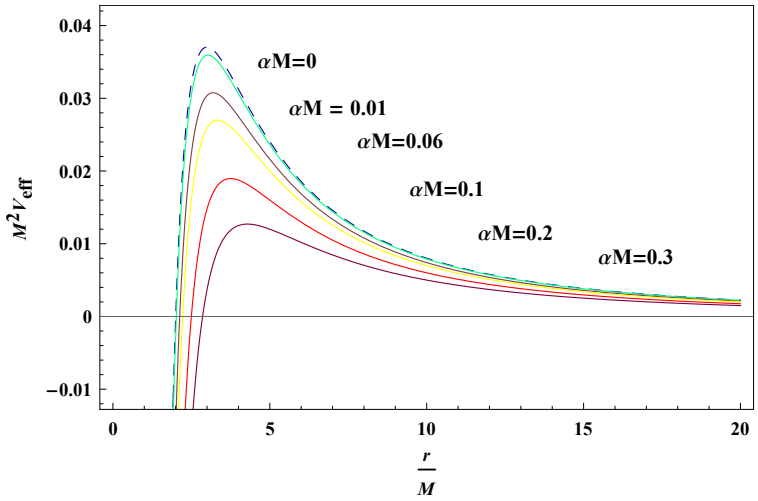

Figure 2.3: The graph of M^2V_{eff} against $\frac{r}{M}$ exhibits unstable circular orbits for different values of α.

2.2.2 Timelike Geodesics

For timelike case, we set $\epsilon = 1$. (2.28) gives the angular momentum of the particle as

$$L^2 = \frac{M}{(u_c - \alpha u_c - 3Mu_c^2)}. \tag{2.42}$$

(2.30) gives the energy as

$$E^2 = \frac{(2Mu_c - 1 + \alpha)^2}{(1 - 3Mu_c - \alpha)}. \tag{2.43}$$

From (2.42) figure 2.5 shows the behavior of L^2 against r_c. It is clear that if the radius of the circular orbit decreases the angular momentum of the particle in that orbit increases due to being a conserved quantity. However, if the radius approaches a minimum value the L^2 tends to infinity. Figure 2.4 shows the difference between horizon radii and circular geodesic radii. It is noticed that the difference between $r_{c_{min}}$ and r_h increases for larger values of α. Hence, the difference becomes infinite and particle can escape to infinity when the value of string cloud parameter approaches to unity.

Stability: Consider the geodesic equation (2.18), putting $\epsilon = 1$ in (2.18)

$$\left[\frac{dr}{d\tau}\right]^2 = E^2 - \left[1 + \frac{L^2}{r^2}\right]\left[1 - \frac{2M}{r} - \alpha\right], \tag{2.44}$$

substituting $\tau = \frac{\tilde{\tau}}{L}$, will implies

$$\left(\frac{dr}{d\tilde{\tau}}\right)^2 + V_{eff}(r) = E_{eff}(r), \tag{2.45}$$

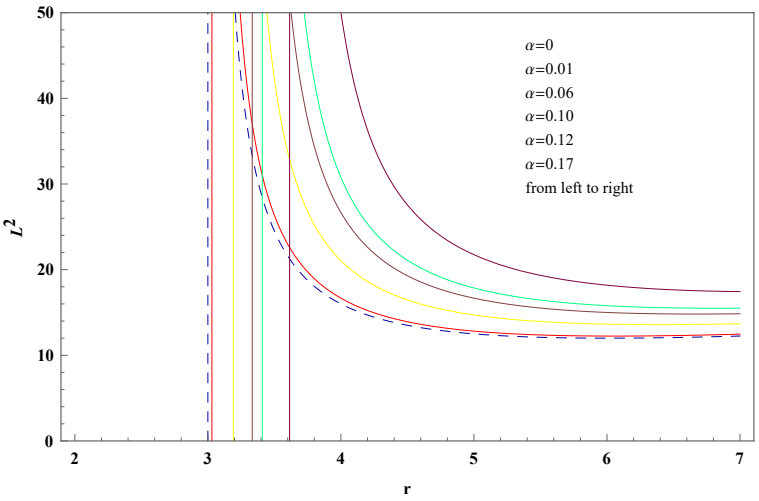

Figure 2.4: Behaviour of angular momentum versus distance for changing α.

here

$$V_{eff}(r) = \left(\frac{1}{r^2} + \frac{1}{L^2}\right)\left(1 - \frac{2M}{r} - \alpha\right), \tag{2.46}$$

$$E_{eff}(r) = \frac{E^2}{L^2}. \tag{2.47}$$

As mentioned before for stable circular orbit V''_{eff} must be positve at critical points.

$$V''_{eff}(r) = \frac{6}{r_c^4} - \frac{24M}{r_c^5} - \frac{4M}{L^2 r^3} - \frac{6\alpha}{r_c^4}, \tag{2.48}$$

putting $V'_{eff} = 0$, gives

$$r_c = \frac{(\alpha - 1)\, L^2 \pm \sqrt{(\alpha - 1)^2\, L^4 - 12M^2 L^2}}{2M}, \tag{2.49}$$

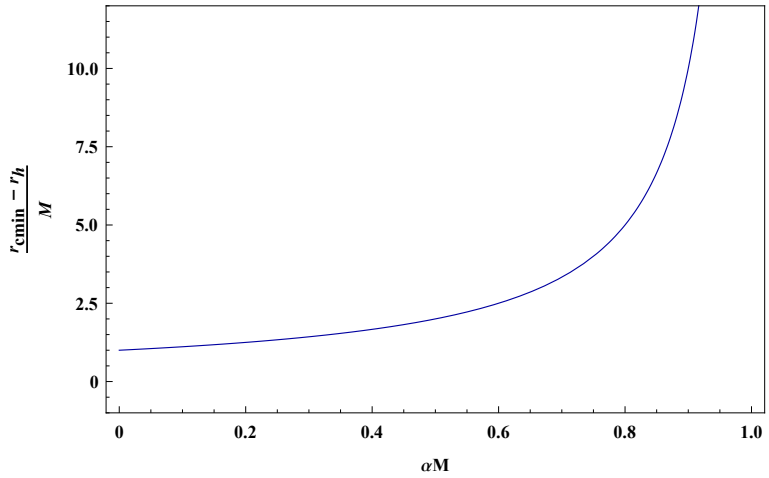

Figure 2.5: The plot of difference between radius of circular orbit and horizon radii against αM.

Plugging the value of r_c in V''_{eff}

$$\begin{aligned} V''_{eff} = 6 &\left(\frac{L^2(\alpha-1) \pm \sqrt{(\alpha-1)^2 L^4 - 12M^2L^2}}{2M} \right)^4 \\ -24M &\left(\frac{L^2(\alpha-1) \pm \sqrt{(\alpha-1)^2 L^4 - 12M^2L^2}}{2M} \right)^5 \\ -\frac{4M}{L^2} &\left(\frac{L^2(\alpha-1)\, L^2 \pm \sqrt{(\alpha-1)^2 L^4 - 12M^2L^2}}{2M} \right)^3 \\ -6\alpha &\left(\frac{L^2(\alpha-1) \pm \sqrt{(\alpha-1)^2 L^4 - 12M^2L^2}}{2M} \right)^4 . \end{aligned} \tag{2.50}$$

Note that the minima of the effective potential are the points where circular orbits are stable and the points where effective potential possesses maxima correspond to unstable orbits. Figure 2.6, 2.7 and 2.8 has shown effective potential for $\alpha = 0.01$, $\alpha = 0.1$, and $\alpha = 0.25$ respectively. Effective potential possesses extrema at different values of r_c. The five different curves of V_{eff} depend on the angular momentum.

In Figure 2.6, the effective potential graph displays maxima at specific values of r (4.4, 4.0, 3.8, and 3.7) for different angular momentum values (14, 16, 18, and 20). Additionally,

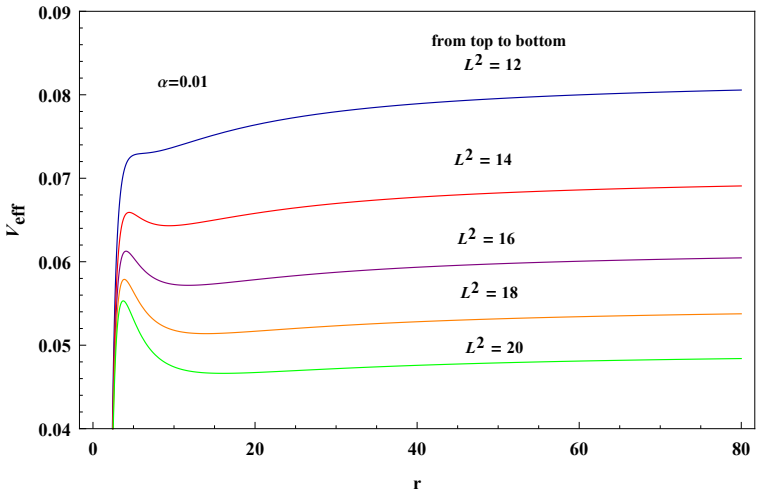

Figure 2.6: The plot of V_{eff} against r shows stable and unstable orbits when $\alpha = 0.01$.

there are minima at other values of r (9.3, 11.7, 13.9, and 16) when α is set to 0.01. These minima indicate the presence of stable circular orbits for massive particles. Moving to Figure 2.7, where α is set to 0.1, there are stable circular orbits at r values of 9.1, 11.5, and 13.5 for angular momentum values of 16, 18, and 20. However, there are also unstable orbits at r values of 5.2, 4.6, and 4.4. In Figure 2.8, there are no stable circular orbits observed for the angular momentum values used, and the graph of the effective potential becomes asymptotically constant. From the observations made, it is concluded that unstable circular orbits for massive particles exist for smaller angular momentum values and larger values of the string cloud parameter (α).

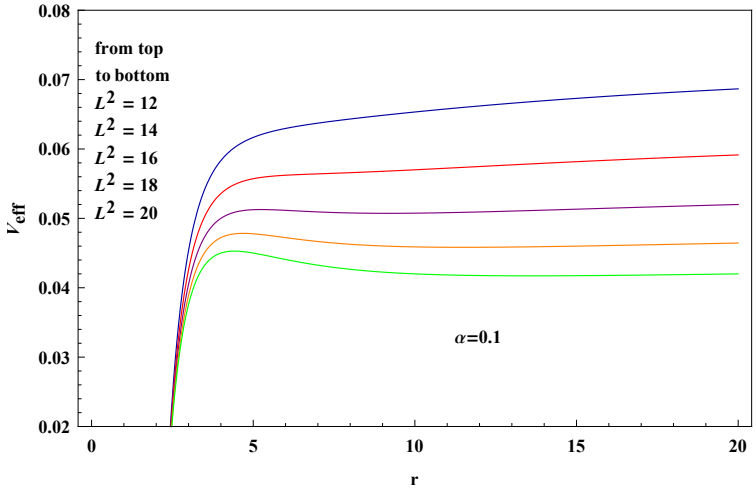

Figure 2.7: The plot of V_{eff} against r indicates stable and unstable orbits when $\alpha = 0.1$.

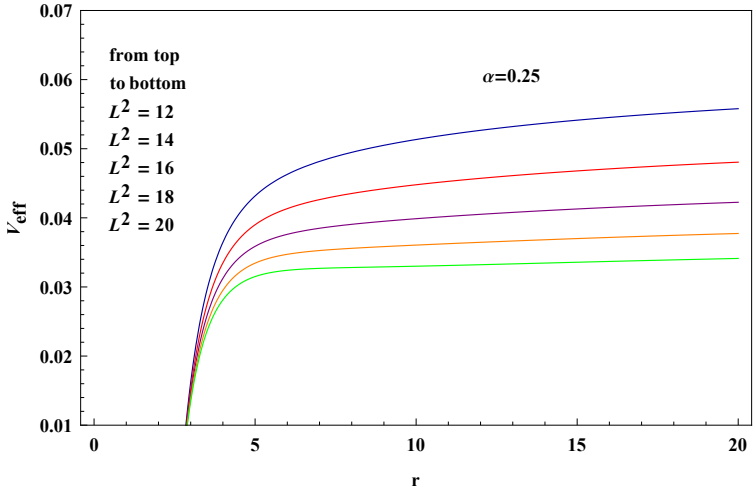

Figure 2.8: The plot of V_{eff} against r indicates unstable orbits when $\alpha = 0.25$.

Chapter 3

Motion of a Particle in the Spacetime Field of the Reissner-Nordström Black Hole with Euler-Heisenberg Parameter

The Universe we are living in is filled with matter and energy. After billions of years since its formation, humans have only been able to access approximately 5% of universe through observations and theories. The rest 95% consists 27% of dark matter (DM) and 68% of dark energy (DE) [29, 30]. These dark components are part of the theory known as "dark universe" theory. The luminous galaxies and groups and rich clusters of galaxies contain huge amount of invisible "dark matter". The existence of the DM component is inferred from the high-velocity dispersion and gas temperature in clusters of galaxies and the high rotation speed of gas and stars in the outer parts of spiral galaxies [31]. DM (probably) has properties that are closest to those of ordinary matter. It is also thought to be responsible to form structures during the period of matter dominance in the history of Universe. DM shares the clustering qualities of ordinary matter but it does not interact with the Standard Model of Particle Physics (SM) gauge bosons (such as electromagnetic ones) [32]. DM obeys strong energy condition (SEC)similar to ordinary matter. Whereas "dark energy" is believed to be the reason behind the recent acceleration in the expansion of the universe, which has been observed through various cosmological and astrophysical measurements, such as the cosmic microwave background (CMB) and type-Ia supernovae [33]. DE is quite unique and different from ordinary matter and dark matter. Unlike them, dark energy does not have the ability to form clusters or structures because it does not satisfy SEC [32].

Evidence for the existence of DM can be observed on various scales, from the cosmic scale down to the astrophysical (galactic and subgalactic) scales. On the other hand,

evidence for DE is less direct and is mainly based on cosmological observations. This distinction is interesting because it suggests that the universe experiences acceleration in its early stages and in the present time as well, indicating the need for additional cosmic components beyond what is currently understood. These additional components may include one or more types of dark matter, inflaton fields (related to cosmic inflation), and some form of dark energy. This suggests that our current understanding of cosmology, known as concordance cosmology, requires the inclusion of these potentially hidden elements to fully explain the universe [32].

The limitations of GR have been completely revealed with the recent rise of the "dark universe" notion as DM and DE are inferred due to their interaction with gravity hence there are now more compelling reasons to modify GR theory. There is a tight relation between DM/DE interaction and the modified theories of gravity. For example, in f(R) gravity the non-relativistic matter is universally connected to a scalar field after carrying out a conformal transformation from Jordan frame to Einstein frame so that the scalar field can act as DE [33]. Hence, the modified gravity theories seem highly promising, especially in light of the fact that gravity remains the least understood among the four fundamental forces.

Proposals to expand this theory began to be made in 1919, four years after GR had been developed. Notable examples include Weyl's scale independent theory [34] and Eddington's theory of connections [35]. These early GR modifications were carried out without any formal theoretical or experimental justification and motivated only by scientific curiosity. However, theoretical support for altering gravitational action appeared quite quickly. The fundamental cause was the nonquantizablity of GR in the manner in which conventional Quantum Field Theories are quantized since it was nonrenormalizable. It was established that there must be an addition of higher order curvature components to the Einstein–Hilbert action in order for 1-loop renormalization to take place. In spite of that, all modified GR theories had a common denominator. The terms which were added in gravitational action to modify GR were significant at extremely small scale (Planck scale) and hence, no impact on late universe.

In other words, modifications to GR might offer a consistent explanation for both early and late-time acceleration as well as the DM that seems to pervade the entire cosmos. The "dark universe riddle" can be resolved by modified theories of gravity.

Mimetic gravity is one of the most interesting, modified gravity theories that emerge in recent years. Mimetic gravity, also modified mimetic gravity can describe the dark components of the universe as merely geometric effects without the inclusion of additional

matter fields.

Chamseddine and Mukhanov introduced the term "mimetic dark matter" in a 2013 publication [36] even though a few years earlier the basic framework for mimetic theories was already provided in three separate papers [37–39]. They proposed an idea that aims to separate the conformal degree of freedom of gravity [36]. This was achieved by expressing physical metric $g_{\mu\nu}$ using an an auxiliary metric $\widetilde{g}_{\mu\nu}$ and a scalar field ϕ labeled as mimetic field, given as

$$g_{\mu\nu} = -\widetilde{g}_{\mu\nu}\widetilde{g}^{\rho\sigma}\partial_\rho\phi\partial_\sigma\phi \tag{3.1}$$

physical metric remains unchanged under conformal transformations of the auxiliary metric of type $\widetilde{g} \to \Omega(t,\mathbf{x})^2$, $\Omega(t,\mathbf{x})$ being a function of the spacetime coordinates, as is evident from (3.1). It is also obvious that the mimetic field needs to adhere to the restriction as a consistency condition given as:

$$g^{\mu\nu}\partial_\mu\phi\partial_\nu\phi = -1. \tag{3.2}$$

Heisenberg and Euler formulated the Lagrangian of nonlinear electrodynamics. They used the Dirac theory of electron-positron to construct this non-perturbative one-loop Lagrangian [40]. Later, Schwinger expanded on their work within the framework of Quantum Electrodynamics (QED) [41]. He proved that the phenomenon of vacuum polarization can be explained by using this Lagrangian, where vacuum can undergo changes due to the production of electron-positron pairs in the presence of electric fields which must be strong enough than critical value $E_c = \frac{m^2c^3}{e\hbar}$ [40–42]. For a long time, scientists have been interested in studying electron-positron pair production from the QED vacuum and the vacuum polarization by an external electromagnetic field [43]. Quantum electrodynamics (QED) is a fundamental theory that describes electromagnetic interactions and has been experimentally verified. Given the importance of QED, researchers have been exploring its effects in black hole physics. Therefore, nonlinear electrodynamics described by the Heisenberg-Euler Lagrangian together with the QED has attracted huge attention in the study of generalized black hole solutions. Hence, many interesting studies on black holes using this framework have been presented [42, 44–47]

3.1 Field Equations of Mimetic Euler-Heisenberg Theory

The action of mimetic Euler-Heisenberg theory (MEH) in four dimensions can be expressed as follows [48]

$$\mathcal{S} := \frac{1}{2k}\int \Big[- g(\widetilde{g}_{\alpha\beta},\phi)\Big]^{\frac{1}{2}} d^4x - \int \big[-g(\widetilde{g}_{\alpha\beta},\phi)\Big]^{\frac{1}{2}} \mathcal{L}(\mathcal{F},J)d^4x, \tag{3.3}$$

where $k = 8\pi$, $g(\widetilde{g}_{\alpha\beta},\phi)$ denotes the determinant of the metric tensor, ϕ is a scalar field and $\mathcal{L}(\mathcal{F},J)$ represents the nonlinear electromagnetic Lagrangian. The nonlinear

electromagnetic Lagrangian $\mathcal{L}(\mathcal{F}, J)$ depends on invariants $\mathcal{F}$ and J defined as

$$\mathcal{F} = \frac{1}{4}\mathcal{F}_{\mu\nu}\mathcal{F}^{\mu\nu}, \quad J = \frac{1}{4}\mathcal{F}_{\mu\nu}{}^{\star}\mathcal{F}^{\mu\nu}, \tag{3.4}$$

here, $\mathcal{F}_{\mu\nu}$ represents the electromagnetic field strength tensor, and ${}^{\star}\mathcal{F}^{\mu\nu}$ denotes the dual of $\mathcal{F}_{\mu\nu}$ defined as ${}^{\star}\mathcal{F}^{\mu\nu} := \frac{\sqrt{-g(\widetilde{g}_{\alpha\beta},\phi)}}{2}\epsilon^{\alpha\beta\mu\nu}\mathcal{F}_{\alpha\beta}$, where $\epsilon_{\alpha\beta\gamma\delta}$ is a completely skew-symmetric tensor satisfying following condition

$$\epsilon^{\alpha\beta\gamma\delta}\epsilon_{\alpha\beta\gamma\delta} = -4!.$$

The nonlinear electromagnetic field Lagrangian is expressed as [48]

$$\mathcal{L}\big(\mathcal{F}, J\big) := -\mathcal{F} + \frac{\mu}{2}\mathcal{F}^2 + \frac{7\mu}{8}J^2, \tag{3.5}$$

In (3.5), μ is the EH parameter that controls the intensity of the nonlinear electromagnetic contribution and is given by $\mu = \frac{8\alpha^2}{45M^2}$, where α is the fine structure constant and M is the mass of the central particle so that the EH parameter is of order $\frac{\alpha}{E_c^2}$, where E_c denotes the electric field strength. The fine structure constant characterizes the strength of electromagnetic interaction between charged particles and is approximately equal to $\frac{1}{137.036}$. It can be noticed that larger values of μ can increase the nonlinearity of electromagnetic field while, by choosing smaller values of μ the effects of nonlinear terms can be reduced. The EH theory originally considers μ to be positive.

When $\mu = 0$, the Lagrangian reduces to Maxwell electrodynamics, where $\mathcal{L}\mathcal{F} = -\mathcal{F}$. There are two possible frames in the context of nonlinear electromagnetism, the classical frame and the K-frame. In classical frame, the $\mathcal{F}$ can be used in terms of electromagnetic field tensor $\mathcal{F}_{\mu\nu}$. On the other hand, in the K-frame, tensor $\mathcal{K}^{\mu\nu}$ being the main field is expressed as

$$K^{\mu\nu} := -\left(\mathcal{L}_{\mathcal{F}}\mathcal{F}^{\mu\nu} + {}^{\star}\mathcal{F}^{\mu\nu}\mathcal{L}_J\right), \tag{3.6}$$

here $\mathcal{L}_{\mathcal{F}}$ and $\mathcal{L}_J$ represents the derivative of $\mathcal{L}$ w.r.t. $\mathcal{F}$ and J respectively. In the context of MEH theory, $K^{\mu\nu}$ can be expressed as

$$K^{\mu\nu} := (1 - \mu\mathcal{F})\,\mathcal{F}^{\mu\nu} - \frac{7\mu}{4}{}^{\star}\mathcal{F}^{\mu\nu}J. \tag{3.7}$$

The fundamental relationships between the electric field E, electric induction $\mathcal{D}$, magnetic field $\mathcal{H}$ and magnetic intensity $\mathcal{B}$, in the context of EH nonlinear electromagnetism is expressed in (3.7). In the K-frame, two invariants denoted as K and O are given by:

$$K = \frac{1}{4}K_{\mu\nu}\mathcal{F}^{\mu\nu}, \qquad O = -\frac{1}{4}K^{\star}_{\mu\nu}K^{\mu\nu}, \tag{3.8}$$

where

$$^{\star}K_{\mu\nu} = \frac{1}{2\sqrt{-g(\widetilde{g}_{\mu\nu},\phi)}}\epsilon_{\mu\nu\gamma\lambda}K^{\gamma\lambda}.$$

By utilizing the information provided above, we can derive the field equations of the MEH theory as

$$G_{\mu}{}^{\nu} = T_{\mu}^{EH\nu} - \widetilde{T}_{\mu}{}^{\nu}, \qquad \nabla_{\mu}K^{\mu\nu} = 0, \tag{3.9}$$

where $G_{\mu\nu}$, $\widetilde{T}_{\mu\nu}$ and $T_{\mu}{}^{\nu EH}$ represents the Einstein tensor, energy-momentum tensor of the mimetic field and the energy-momentum tensor of the MEH theory respectively, in the K-frame. The specific form of $T_{\mu}{}^{\nu EH}$ is provided as

$$T^{EH}{}_{\mu}{}^{\nu} = \frac{1}{4\pi}\left(\Big[1-\mu K\Big]K^{\alpha}{}_{\mu}K_{\nu\alpha} + \delta_{\mu}{}^{\nu}\Big[K - \frac{3}{2}\mu K^2 - \frac{7\mu}{8}O^2\Big]\right). \tag{3.10}$$

Notice that the MEH field equations involve the auxiliary metric, which is implicitly incorporated through the physical metric specified in (3.2) and the mimetic field ϕ. The inclusion of the mimetic field in the field equations is expressed as

$$\widetilde{T}_{\mu\nu} = -\left(G - T^{EH}\right)\partial_{\mu}\phi\partial_{\nu}\phi, \tag{3.11}$$

where $G = -R$ is the trace of the Einstein tensor. It is noteworthy that energy-momentum tensors, $T^{EH}{}_{\alpha\beta}$ and $\widetilde{T}_{\alpha\beta}$ are conserved. Therefore, they satisfy the continuity equations

$$\nabla^{\alpha}\widetilde{T}_{\alpha\beta} = 0 = \nabla^{\alpha}T^{EH}{}_{\alpha\beta}, \tag{3.12}$$

∇^{α} represents the covariant derivative. Taking into account the mimetic field condition given in (3.2) and the energy-momentum tensor in (3.11), corresponding continuity becomes

$$\nabla^{\mu}\left(G - T^{EH}\partial_{\mu}\phi\right) = \frac{1}{\sqrt{-g}}\partial_{\mu}\left(\sqrt{-g}\left[G - T^{EH}\right]g^{\mu\sigma}\partial_{\sigma}\phi\right) = 0, \tag{3.13}$$

which is obtained by varying the action (3.3) w.r.t the mimetic scalar field ϕ. If (3.2) is used, it can be observed that (3.13) is satisfied identically. It can be easily shown that the trace of (3.9) takes the following form

$$\left[G - T^{EH}\right]\left(1 + g^{\alpha\beta}\partial_{\alpha}\phi\partial_{\beta}\phi\right) \equiv 0, \tag{3.14}$$

It is concluded that the conformal degree of freedom provides a dynamical quantity, particularly if $G \neq 0$ This means that the mimetic theory possesses non-trivial solutions for the conformal mode even in the absence of matter [36].

3.1.1 Charged Mimetic Euler-Heisenberg Black Hole Solution

In the current section, the field equations of the MEH theory are applied to a spherically symmetric spacetime. To do so, consider the metric:

$$ds^2 = f_1(r)dt^2 - \frac{dr^2}{f_2(r)} - r^2\big(d\theta^2 + r^2\sin^2\theta d\phi^2\big), \tag{3.15}$$

where $f_1(r)$ and $f_2(r)$ are unknown functions. These functions are determined by using the MEH field equations. The following nonlinear differential equations are obtained when the field equations are applied to the spacetime (3.15).
The (t,t)-component of the MEH equation is given as [48]

$$\frac{1}{128r^2f_1^6}\Bigg[128f_1^6\Big[1-rf_2'-f_2\Big] - q'^2f_2r^2\Big[64f_1^5$$

$$+\mu\Big(48q'^2f_2f_1^4 - 16\mu f_1^3f_2^2q'^4 - 24\mu^2f_1^2f_2^3q'^6 - 8\mu^3f_1f_2^4q'^8 - \mu^4f_2^5q'^{10}\Big)\Big]\Bigg] = 0, \tag{3.16}$$

the (r,r)-component takes the following form

$$\frac{1}{128r^2f_1^6}\Bigg(128f_1^5\Big[f_1 - f_1f_2 - rf_2f_1'\Big]$$

$$-4\psi'^2f_2\Big[32f_2f_1^5r^2f_1'' + q'^2r^2\mu\Big(16q'^2f_2f_1^4 + 32\mu f_1^3f_2^2q'^4 + 24\mu^2f_1^2f_2^3q'^6 + 8\mu^3f_1f_2^4q'^{10}\Big)$$

$$+16f_1^4\Big(rf_1f_1'\Big[4f_2 + rf_2'\Big] - r^2f_2f_1'^2 + 4f_1^2\Big[f_2 - 1 + rf_2'\Big]\Big)\Big]$$

$$-q'^2f_2r^2\Big[64f_1^5+\mu\Big(48q'^2f_2f_1^4-16\mu {f_2}^2f_1^3q'^4-24\mu^2f_1^2f_2^3q'^6-8\mu^3f_1f_2^4q'^8-\mu^4f_2^5q'^{10}\Big)\Big]\Bigg) = 0, \tag{3.17}$$

the (θ,θ) and (ϕ,ϕ)-components are expressed as,

$$\frac{1}{128rf_1^6}\Big(32f_1^4\Big[rf_2f_1'^2 - f_-1f_1'\Big[2f_2 + rf_2'\Big]r^2 - 2f_1^2f_2'\Big]$$

$$-64rf_1^5f_1f_1''+q'^2f_2r\Big[64f_1^5+\mu\Big(16q'^2f_1^4-80\mu f_1^3f_2^2q'^4-72\mu^2f_1^2f_2^3q'^6-24\mu^3f_1f_2^4q'^8-3\mu^4f_2^5q'^{10}\Big)\Big]\Big) = 0, \tag{3.18}$$

the nonlinear charged field equation is

$$-\frac{2rf_2f_1q''\Big(2f_1+3\mu f_2q'^2\Big)+q'\Big(q'^{\mu}f_2 3rf_1f_2'+f_2\Big[4f_1-3rf_1'\Big]+2f_1\Big[rf_1f_2'\Big]+f_2\Big(4f_1-rf_1'\Big)\Big)\Big]\Big)}{4rf_1^3}=0, \tag{3.19}$$

where $q \equiv q(r)$ being an unknown function is associated with the electric field. It is defined through the vector potential

$$U = q(r)dt, \tag{3.20}$$

whereas $q' = \dfrac{dq}{dr}$. The previously described nonlinear differential equations (3.18) and (3.19) are solved for the case $f_1(r) = f_2(r)$. The analytic solution of the nonlinear differential equations (3.18) and (3.19) is obtained as

$$f_1(r) = 1 + \frac{c}{r} + \frac{{c_1}^2}{8r^2} - \frac{{c_1}^4\mu}{640r^6}, \tag{3.21}$$

$$\begin{aligned} q(r) &= \int \frac{2\sqrt[3]{18\mu^3r^2\Big(9c_1\sqrt{\mu}+\sqrt{3(32r^4+27c_1^2\mu)}\Big)^2}-24r^2\mu}{6r\mu^3\sqrt{r\mu\Big(108c_1\mu+12\sqrt{3\mu(32r^4+27{c_1}^2\mu)}\Big)}}\,dr + c_2 \\ &\approx c_2 - \frac{c_1}{2r} + \frac{\mu c_1^3}{80r^5} - \frac{\mu^2c_1^5}{384r^9} + \frac{3\mu^3c_1^7}{3328r^{13}} - O\Big(\frac{1}{r^{17}}\Big) + \cdots . \end{aligned} \tag{3.22}$$

Note that on substituting $\mu = 0$, we return to the RN solution. The mimetic field is

$$\begin{aligned} \phi &= 8\int \sqrt{\frac{10r^6}{80{c_1}^2r^4} - \mu{c_1}^4 + 640r^5\Big(r+c\Big)}\,dr \\ &\approx r - \frac{1}{2}c\ln(r) + \frac{{c_1}^2-6c^2}{16r} + \frac{c\Big(10c^2-3{c_1}^2\Big)}{64r^2} + O\frac{1}{r^3} + \cdots . \end{aligned} \tag{3.23}$$

The spacetime metric is expressed as follows

$$ds^2 = \Big(1-\frac{2M}{r}+\frac{q^2}{r^2}-\frac{q^4\mu}{10r^6}\Big)dt^2 - \frac{dr^2}{\Big(1-\dfrac{2M}{r}+\dfrac{q^2}{r^2}-\dfrac{q^4\mu}{10r^6}\Big)} - r^2\Big(d\theta^2+\sin^2\theta d\phi^2\Big), \tag{3.24}$$

where $c = -2M$ and $c_1 = \sqrt{8}q$.

Note: We consider the spacetime (3.24) with signature $(-,+,+,+)$ as we follow this signature throughout the dissertation.

$$ds^2 = -\Big(1-\frac{2M}{r}+\frac{q^2}{r^2}-\frac{q^4\mu}{10r^6}\Big)dt^2 + \frac{dr^2}{\Big(1-\dfrac{2M}{r}+\dfrac{q^2}{r^2}-\dfrac{q^4\mu}{10r^6}\Big)} + r^2\Big(d\theta^2+\sin^2\theta d\phi^2\Big). \tag{3.25}$$

The horizon of (3.25) are obtained by

$$f(r) = 1 - \frac{2M}{r_h} + \frac{q^2}{r_h^2} - \frac{q^4\mu}{10r_h^6} = 0. \tag{3.26}$$

which yields

$$r_h = 1.9949. \tag{3.27}$$

where $M = 1$, $q = 0.1$ and $\mu = 9.46691 \times 10^{-6}$. There is only one horizon whose radius is $r_{h2} = 1.9949$. It is worth noting that RN black hole has two horizons, the outer horizon is same for both cases i,e $r_h = 1.9949$, but inner horizon vanished in new case.

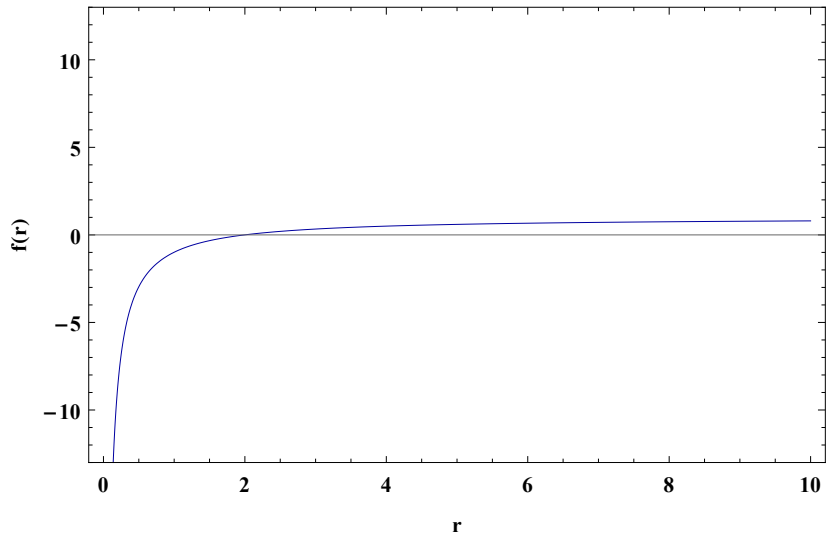

Figure 3.1: The event horizon is obtained by plotting $f(r)$ against r.

In Figure (3.2), red curve indicates event horizon in RN case and blue curve represents event horizon in Euler-Heisenberg case. It is clear that inner horizon disappeared in EH case.

In the upcoming section, the trajectories of the massive and massless particles for the circular motion will be derived using Lagrangian formalism. We will discuss stable and unstable circular orbits of the particles.

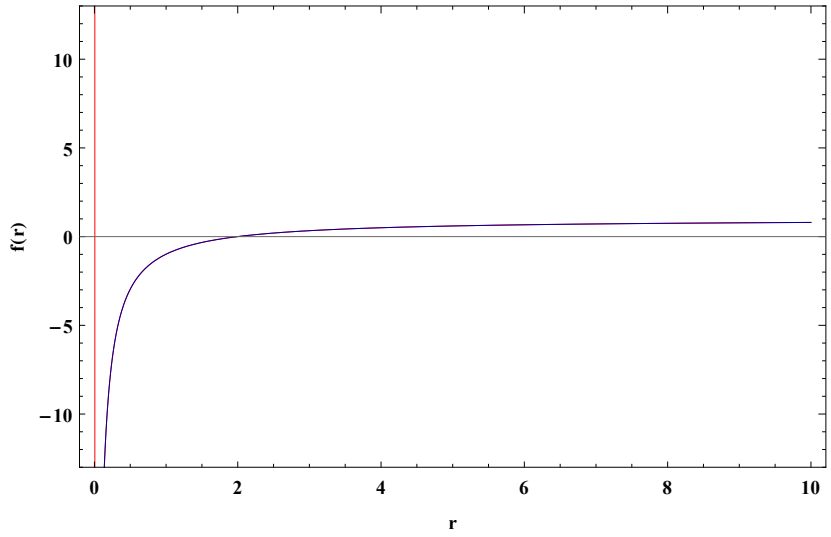

Figure 3.2: A comparison between horizons of RN black hole without and with EH parameter. Red curve represents RN black hole when $\mu = 0$.

3.2 Particle Trajectories

The geodesics Lagrangian is given as

$$\mathcal{L} = \frac{m}{2} g_{\mu\nu} \dot{x}^\mu \dot{x}^\nu = m\bigg(-\frac{1}{2} f(r) \dot{t}^2 + \frac{\dot{r}^2}{2f(r)} + \frac{1}{2} r^2 \Big(\dot{\theta}^2 + \sin^2\theta \dot{\phi}^2 \Big) \bigg). \tag{3.28}$$

The EL equations are

$$\frac{d}{d\lambda}\Big(\frac{\partial \mathcal{L}}{\partial \dot{x}^\eta}\Big) - \frac{\partial \mathcal{L}}{\partial x^\eta} = 0, \quad (\eta = 0, 1, 2, 3) \tag{3.29}$$

For $\eta = 0$, (3.29) gives,

$$-f(r)\dot{t} = \text{constant} = \frac{e}{m} = E, \tag{3.30}$$

$$\dot{t} = \frac{e}{f(r)m} = \frac{-E}{f(r)}, \tag{3.31}$$

where

$$f(r) = 1 - \frac{2M}{r} + \frac{q^2}{r^2} - \frac{q^4\mu}{10r^6}, \tag{3.32}$$

which implies

$$\dot{t} = \frac{-E}{\Big(1 - \frac{2M}{r} + \frac{q^2}{r^2} - \frac{q^4\mu}{10r^6}\Big)}. \tag{3.33}$$

For η=3,

$$\frac{d}{d\lambda}\Big(\frac{\partial \mathcal{L}}{\partial \dot{\phi}}\Big) - \frac{\partial \mathcal{L}}{\partial \phi} = 0, \tag{3.34}$$

$$\frac{\partial \mathcal{L}}{\partial \phi} = 0, \implies \frac{d}{d\lambda}\Big(\frac{\partial \mathcal{L}}{\partial \dot{\phi}}\Big) = 0, \tag{3.35}$$

$$\dot{\phi} r^2 \sin^2\theta = \text{constant} = \frac{l}{m} = L, \tag{3.36}$$

$$\dot{\phi} = \frac{L}{r^2 \sin^2\theta}. \tag{3.37}$$

In (3.30) E stands for conserved energy while in (3.36) L for angular momentum of the particle. As the particle is moving in equatorial plane where we take $\theta = \frac{\pi}{2}$. Hence $L = r^2\dot{\phi}$.
Since the normalization condition for four-velocity is

$$g_{\mu\nu}\frac{dx^\mu}{d\lambda}\frac{dx^\nu}{d\lambda} = -\epsilon. \tag{3.38}$$

In the equatorial plane, (3.38) implies

$$-\Big(1 - \frac{2M}{r} + \frac{q^2}{r^2} - \frac{q^4\mu}{10r^6}\Big)\dot{t}^2 + \frac{\dot{r}^2}{\Big(1 - \frac{2M}{r} + \frac{q^2}{r^2} - \frac{q^4\mu}{10r^6}\Big)} + r^2\dot{\phi}^2 = -\epsilon, \tag{3.39}$$

using (3.33) and (3.37) in (3.39) we get

$$\Big(\frac{dr}{d\lambda}\Big)^2 = E^2 - \Big(1 - \frac{2M}{r} + \frac{q^2}{r^2} - \frac{q^4\mu}{10r^6}\Big)\Big(\epsilon + \frac{L^2}{r^2}\Big), \tag{3.40}$$

$$\frac{1}{2}\Big(\frac{dr}{d\lambda}\Big)^2 + V_{eff}(r) = \frac{1}{2}E^2. \tag{3.41}$$

here $V_{eff}(r) = \frac{1}{2}\Big(1 - \frac{2M}{r} + \frac{q^2}{r^2} - \frac{q^4\mu}{10r^6}\Big)\Big(\epsilon + \frac{L^2}{r^2}\Big)$, denotes the effective potential and the corresponding effective energy is

$$E_{eff} = \frac{1}{2}E^2. \tag{3.42}$$

3.3 Circular Motion

In circular motion the radial coordinate r is constant which implies that the $\dot{r}$ and $\ddot{r}$ are equal to zero. For the sake of simplicity, we introduce a new variable u defined as $r = \dfrac{1}{u}$. We consider the condition $\dfrac{du}{d\phi} = 0$ at $u = u_c$, where $r_c = \dfrac{1}{u_c}$ represents the radius of the

circular orbit of the particle.
The chain rule implies

$$\dot{r} = \frac{dr}{d\xi} = \frac{dr}{d\phi}\frac{d\phi}{d\xi} = \frac{L}{r^2}\frac{dr}{d\phi}, \tag{3.43}$$

(3.40) becomes

$$\left(\frac{du}{d\phi}\right)^2 = \frac{E^2}{L^2} - \left(1 - 2Mu + q^2u^2 - \frac{q^4\mu}{10}u^6\right)\left(u^2 + \frac{\epsilon}{L^2}\right), \tag{3.44}$$

$$\left(\frac{du}{d\phi}\right)^2 = \frac{E^2}{L^2} - u^2 + 2Mu^3 - q^2u^4 + \frac{q^4\mu}{10}u^8 - \frac{\epsilon}{L^2} + \frac{2M\epsilon}{L^2}u - \frac{q^2\epsilon}{L^2}u^2 + \frac{q^4\mu\epsilon}{10L^2}u^6. \tag{3.45}$$

Differentiating both sides with respect to ϕ

$$\frac{d^2u}{d\phi^2} = -u + 3Mu^2 - 2q^2u^3 + \frac{2}{5}q^4\mu u^7 + \frac{M\epsilon}{L^2} - \frac{q^2\epsilon}{L^2}u + \frac{3}{10}\frac{q^4\mu\epsilon}{L^2}u^5, \tag{3.46}$$

at $u = u_c$

$$\frac{E^2}{L^2} - \left(1 - 2Mu_c + q^2u_c^2 - \frac{q^4\mu}{10}u_c^6\right)\left(u_c^2 + \frac{\epsilon}{L^2}\right) = 0. \tag{3.47}$$

Since we have $\frac{d^2u}{d\phi^2} = 0$ for the circular motion, implies (3.47) takes the form

$$\frac{d}{du}\left[\frac{E^2}{L^2} - \left(1 - 2Mu + q^2u^2 - \frac{q^4\mu}{10}u^6\right)\left(u^2 + \frac{\epsilon}{L^2}\right)\right]_{u=u_c} = 0. \tag{3.48}$$

These conditions lead to the expression for L^2 as

$$-u_c + 3Mu_c^2 - 2q^2u_c^3 + \frac{2}{5}q^4\mu u_c^7 + \frac{M\epsilon}{L^2} - \frac{q^2\epsilon}{L^2}u_c + \frac{3}{10}\frac{q^4\mu\epsilon}{L^2}u_c^5 = 0, \tag{3.49}$$

solving for L^2 gives

$$L^2 = \frac{M\epsilon - q^2\epsilon u_c + \frac{3q^4\mu\epsilon}{10}u_c^5}{u_c - 3Mu_c^2 + 2q^2u_c^3 - \frac{2q^4\mu}{5}u_c^7}. \tag{3.50}$$

Energy of the particle: Multiplying (3.47) by L^2 yields

$$E^2 = \left(1 - 2Mu_c + q^2u_c^2 - \frac{q^4\mu}{10}u_c^6\right)\left(\epsilon + L^2u_c^2\right). \tag{3.51}$$

Substituting (3.50) in (3.51)

$$E^2 = \frac{1}{\left(u_c - 3Mu_c^2 + 2q^2u_c^3 - \frac{2q^4\mu}{5}u_c^7\right)}\left[\left(\epsilon - 2M\epsilon u_c + q^2\epsilon u_c^2 - \frac{q^4\mu\epsilon}{10}u_c^6\right)\left(u_c - 3Mu_c^2 + 2q^2u_c^3 - \frac{2q^4\mu}{5}u_c^7\right)\right.$$
$$\left. + \left(u_c^2 - 2Mu_c^3 + q^2u_c^4 - \frac{q^4\mu}{10}u_c^8\right)\left(M\epsilon - q^2\epsilon u_c + \frac{3q^4\mu\epsilon}{10}u_c^5\right)\left(u_c - 3Mu_c^2 + 2q^2u_c^3 - \frac{2q^4\mu}{5}u_c^7\right)\right], \tag{3.52}$$

or

$$E^2=\frac{\epsilon}{\left(u_c-3Mu_c^2+2q^2u_c^3-\frac{2q^4\mu}{5}u_c^7\right)}\Bigg[u_c-4Mu_c^2+\left(q^2+4M^2\right)u_c^3-4Mq^2u_c^4+q^4u_c^5-\frac{2}{10}q^4\mu{u_c}^7 \\ +\frac{4}{10}Mq^4\mu{u_c}^8-\frac{2}{10}q^6\mu{u_c}^9+\frac{1}{100}q^8\mu^2\epsilon{u_c}^{13}\Bigg]. \tag{3.53}$$

Since $u_c=\dfrac{1}{r_c}$,

$$E^2=\frac{\frac{\epsilon}{r_c^{13}}\left[r_c^{12}-4Mr_c^{11}+\left(q^2+4M^2\right)r_c^{10}-4Mq^2r_c^9+q^4r_c^8-\frac{2}{10}q^4\mu r_c^6+\frac{4}{10}Mq^4\mu r_c^5-\frac{2}{10}q^6\mu r_c^4+\frac{1}{100}q^8\mu^2\right]}{\frac{1}{r_c^7}\left[r_c^6-3Mr_c^5+2q^2r_c^4-\frac{2}{5}q^4\mu\right]}. \tag{3.54}$$

3.3.1 Timelike Geodesics

We set $\epsilon=1$ for timelike geodesics. For physically acceptable motion, the energy of the particle should be positive. The simplified form of (3.53) is obtained as

$$E^2=\frac{1}{\left(u_c-3Mu_c^2+2q^2u_c^3-\frac{2q^4\mu}{5}u_c^7\right)}\Bigg[u_c-4Mu_c^2+\left(q^2+4M^2\right)u_c^3-4Mq^2u_c^4+q^4u_c^5-\frac{2}{10}q^4\mu{u_c}^7 \\ +\frac{4}{10}Mq^4\mu{u_c}^8-\frac{2}{10}q^6\mu{u_c}^9+\frac{1}{100}q^8\mu^2\epsilon{u_c}^{13}\Bigg], \tag{3.55}$$

since $u_c=\frac{1}{r_c}$

$$E^2=\frac{\frac{1}{r_c^{13}}\left[r_c^{12}-4Mr_c^{11}+\left(q^2+4M^2\right)r_c^{10}-4Mq^2r_c^9+q^4r_c^8-\frac{2}{10}q^4\mu r_c^6+\frac{4}{10}Mq^4\mu r_c^5-\frac{2}{10}q^6\mu r_c^4+\frac{1}{100}q^8\mu^2\right]}{\frac{1}{r_c^7}\left[r_c^6-3Mr_c^5+2q^2r_c^4-\frac{2}{5}q^4\mu\right]}. \tag{3.56}$$

$E^2>0$ for region:

$$r_c>2.99332, \tag{3.57}$$

as shown in figure (3.3).

The expression $\left(u_c-3Mu_c^2+2q^2u_c^3-\dfrac{2q^4\mu}{5}u_c^7\right)$ in E^2 must be greater than zero, this

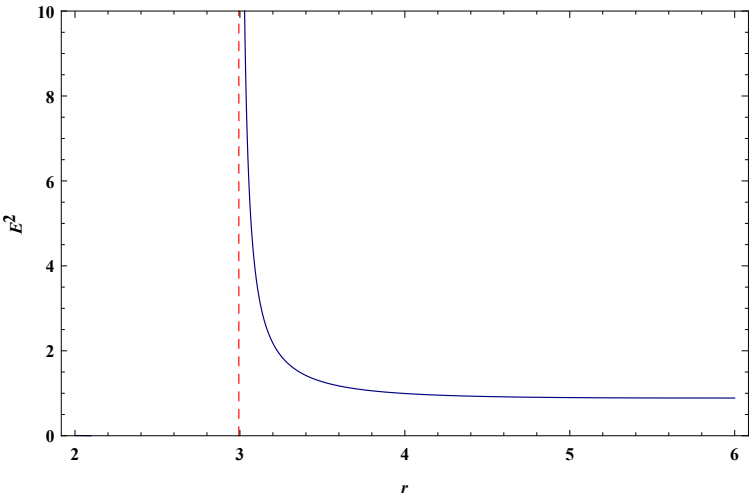

Figure 3.3: The plot of E^2 versus distance indicates region for positive energy.

constraint arises from (3.56) and

$$\frac{1}{r_c^7}\left[r_c^6 - 3Mr_c^5 + 2q^2r_c^4 - \frac{2}{5}q^4\mu\right] > 0, \tag{3.58}$$

$$r_c^6 - 3Mr_c^5 + 2q^2r_c^4 - \frac{2}{5}q^4\mu = 0. \tag{3.59}$$

(3.59) gives minimum radius of circular orbit as $r_{c_{min}} = 2.99332$.

Hence, the geodesic equation $L = r^2\dot{\phi}^2$ cannot be satisfied for circular orbits with $r < 2.99332$. Since they do not satisfy the geodesic equations, these orbits are not geodesics and cannot be followed by freely falling particles. Hence, a particle is unable to set a circular orbit with $r < 2.99332$ around a spherical massive body.

For timelike geodesics, the angular momentum is

$$L^2 = \frac{M - q^2u_c + \frac{3q^4\mu}{10}u_c^5}{u_c - 3Mu_c^2 + 2q^2u_c^3 - \frac{2q^4\mu}{5}u_c^7}. \tag{3.60}$$

As $r_c = \frac{1}{u_c}$, from (3.60) figure (3.5) shows the behavior of L^2 against r_c. It is clear that if the radius of the circular orbit decreases the angular momentum of the particle in that orbit increases due to being a conserved quantity. However, if the radius approaches a minimum value the L^2 tends to infinity.

Stability: Consider the geodesic equation (3.40),

$$\left(\frac{dr}{d\tau}\right)^2 = E^2 - \left(1 - \frac{2M}{r} + \frac{q^2}{r^2} - \frac{q^4\mu}{10r^6}\right)\left(\epsilon + \frac{L^2}{r^2}\right), \tag{3.61}$$

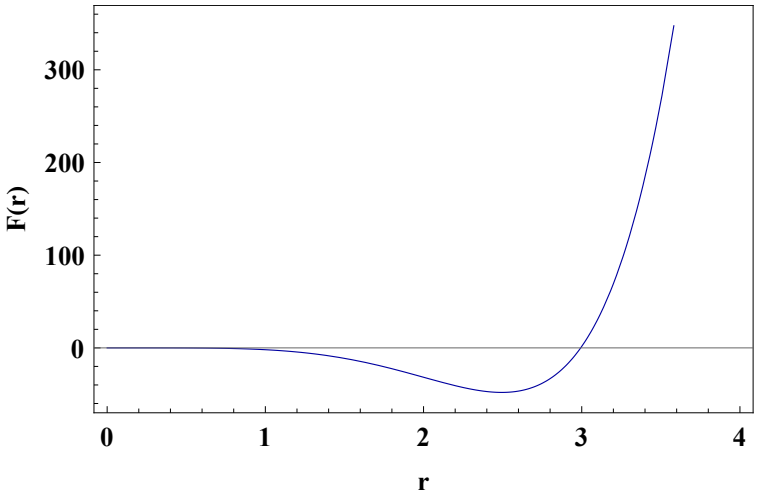

Figure 3.4: The plot of $F(r) = r_c^6 - 3Mr_c^5 + 2q^2r_c^4 - \frac{2}{5}q^4\mu$ versus distance gives minimum radius of circular orbits which indicates $r_{c_{min}} = 2.99332$.

since $\epsilon = 1$

$$\left(\frac{dr}{d\tau}\right)^2 = E^2 - \left(1 - \frac{2M}{r} + \frac{q^2}{r^2} - \frac{q^4\mu}{10r^6}\right)\left(1 + \frac{L^2}{r^2}\right), \tag{3.62}$$

$$\left(\frac{1}{L}\frac{dr}{d\tau}\right)^2 = \frac{E^2}{L^2} - \left(1 - \frac{2M}{r} + \frac{q^2}{r^2} - \frac{q^4\mu}{10r^6}\right)\left(\frac{1}{L^2} + \frac{1}{r^2}\right), \tag{3.63}$$

we consider a substitution $\tau = \dfrac{\tilde{\tau}}{L}$, which implies

$$\left[\frac{dr}{d\tilde{\tau}}\right]^2 + V_{eff}[r] = E_{eff}[r], \tag{3.64}$$

here

$$V_{eff}[r] = \left[1 - \frac{2M}{r} + \frac{q^2}{r^2} - \frac{q^4\mu}{10r^6}\right]\left[\frac{1}{r^2} + \frac{1}{L^2}\right], \tag{3.65}$$

$$E_{eff}[r] = \frac{E^2}{L^2}. \tag{3.66}$$

As mentioned before circular orbit are stable if $\dfrac{dV_{eff}}{dr} = 0$, and $\dfrac{d^2V_{eff}}{dr^2} > 0$, at critical points r_c

$$V_{eff}(r) = \left(1 - \frac{2M}{r} + \frac{q^2}{r^2} - \frac{q^4\mu}{10r^6}\right)\left(\frac{1}{r^2} + \frac{1}{L^2}\right), \tag{3.67}$$

$$V_{eff}(r) = \frac{1}{r^2} - \frac{2M}{r^3} + \frac{q^2}{r^4} - \frac{q^4\mu}{10r^8} + \frac{1}{L^2} - \frac{2M}{rL^2} + \frac{q^2}{r^2L^2} - \frac{q^4\mu}{10r^6L^2}, \tag{3.68}$$

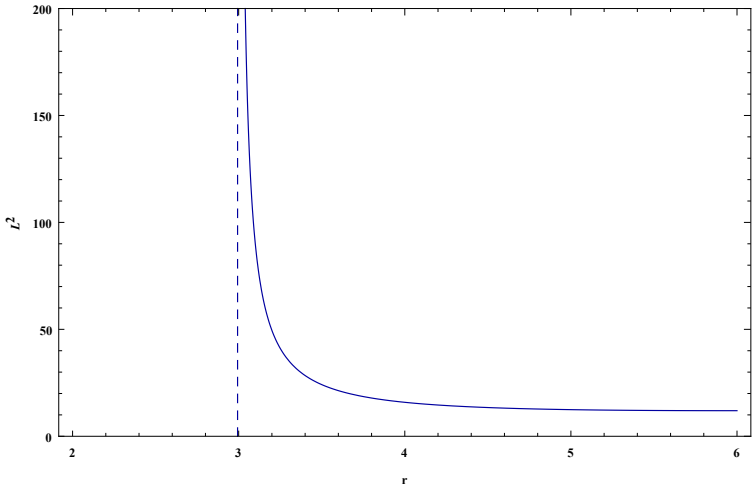

Figure 3.5: Behaviour of L^2 versus r. Here r varies between 0 and 6.

$$V'_{eff}(r) = -\frac{2}{r^3} + \frac{6M}{r^4} - \frac{4q^2}{r^5} + \frac{8}{10}\frac{q^4\mu}{r^9} + \frac{2M}{r^2L^2} - \frac{2q^2}{L^2r^3} + \frac{6}{10}\frac{q^4\mu}{L^2r^7}, \tag{3.69}$$

$$V''_{eff}(r) = \frac{6}{r^4} - \frac{24M}{r^5} + \frac{20q^2}{r^6} - \frac{36}{5}\frac{q^4\mu}{r^{10}} - \frac{4M}{L^2r^3} + \frac{6q^2}{L^2r^4} - \frac{21}{5}\frac{q^4\mu}{L^2r^8}. \tag{3.70}$$

If $L^2 = 12$, then $V'_{eff} = 0$, gives

$$r_{c_1} = 5.68, \tag{3.71}$$

$$r_{c_2} = 6.318. \tag{3.72}$$

Substituting the value of r_{c_1} and r_{c_2} in V''_{eff}

$$V''_{eff}(r_{c_1}) = -0.00397518, \tag{3.73}$$

$$V''_{eff}(r_{c_2}) = 0.000048105. \tag{3.74}$$

We know that the minimum and maximum values of effective potential of a particle correspond to the stable and unstable circular orbits. The effective potential given in (3.67) depends on angular momentum. We can observe the difference in maxima and minima for various values of L^2.

We know that the effective potential of the particle must have minima for stable circular orbits and maximum for unstable orbits. The effective potential given in (3.67) depends on angular momentum. We can observe the difference in maxima and minima for various

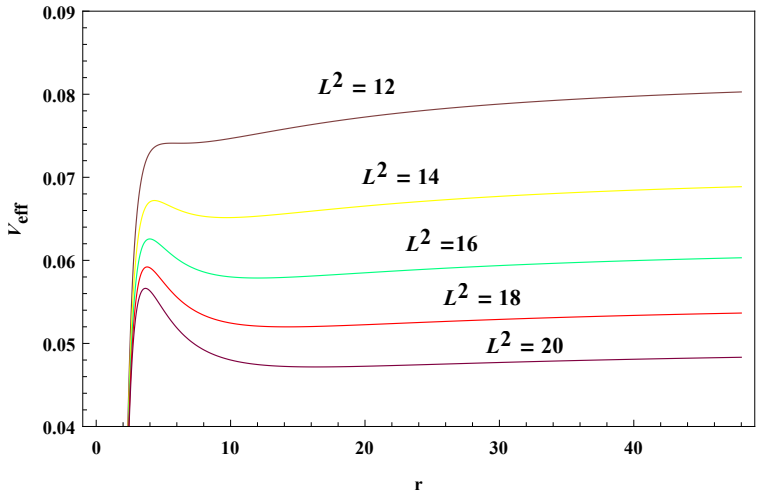

Figure 3.6: Effective potential for massive particles shows stable and unstable circular orbits.

values of L^2. Figure 3.6 illustrates an unstable circular orbit at $r = 5.68$ and a stable orbit at $r = 6.318$ for $L^2 = 12$. Critical points $r = 4.33$ and $r = 9.67$ are obtained when $L^2 = 14$. Here, $V''_{eff} < 0$ at $r = 4.33$ and $V''_{eff} > 0$ at $r = 9.67$ imply unstable and stable orbits, respectively for $L^2 = 14$. The points where circular orbits are stable are $r = 12.01$, $r = 14.21$, $r = 16.34$ while unstable at $r = 3.98$, $r = 3.79$, $r = 3.66$ for $L^2 = 16$, $L^2 = 18$ and $L^2 = 20$ respectively as shown in figure 3.6.

3.3.2 Null Geodesics

For massless particle (3.54) shows that only possible radius for circular photon orbit is

$$r_c^6 - 3Mr_c^5 + 2q^2r_c^4 - \frac{2}{5}\mu q^4 = 0, \tag{3.75}$$

which gives

$$r_c = 2.99332. \tag{3.76}$$

Stability: Consider the geodesic equation (3.40) and a substitution of $\lambda = \frac{\tilde{\tau}}{L}$, implies

$$V_{eff} = \frac{1}{r^2} - \frac{2M}{r^3} + \frac{q^2}{r^4} - \frac{q^4\mu}{10r^8}, \tag{3.77}$$

$$V'_{eff} = -\frac{2}{r_c^3} + \frac{6M}{r_c^4} - \frac{4q^2}{r_c^5} + \frac{8q^4\mu}{10r_c^9}. \tag{3.78}$$

$$V''_{eff} = \frac{6}{r_c^4} - \frac{24M}{r_c^5} + \frac{20q^2}{r_c^6} - \frac{36q^4\mu}{5r_c^{10}}, \tag{3.79}$$

the critical point is

$$r_c = 2.99332, \tag{3.80}$$

at $r_c = 2.99332$, (3.78) becomes

$$V''_{eff} = -0.0248568. \tag{3.81}$$

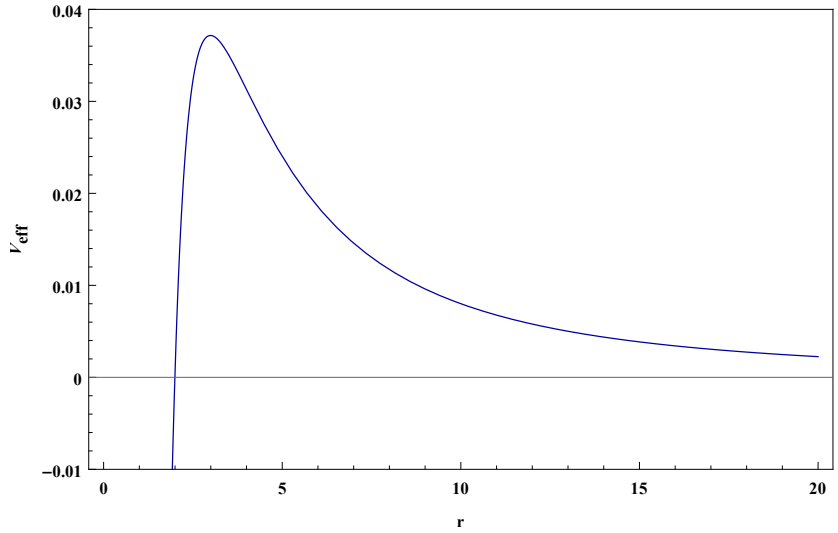

Figure 3.7: The graph of V_{eff} against r for massless particles exhibits unstable circular orbits.

Circular orbits will be stable if they correspond to a minimum of the potential and, unstable if they corresponds to a maximum. We have plotted V_{eff} in figure 3.7 showing that there is no stable circular orbit for photons. This means that photon can orbit forever in this radius where V_{eff} is maximum, but any perturbation can cause it to fly away either to infinity or drop in singularity.

Chapter 4

Summary and Discussion

In this dissertation, we have studied the motion of a neutral particle, near Schwarzschild black hole while considering the presence of electric charge and Euler-Heisenberg parameter which regulates the nonlinearity of electromagnetic field. Timelike and null geodesics for circular motion has been discussed.

The first chapter consisted of some basics of GR. We have discussed the EFEs in the presence of matter, Riemann curvature tensor and its properties, stress-energy tensor and black holes with a couple of examples there.

The second chapter serves as a review of the motion of a particle experiencing the combined effect of gravitational and string cloud parameter forces. Specifically, it focuses on the analysis of geodesics in the Schwarzschild spacetime with string cloud parameter and compares the obtained results with the Schwarzschild case. A significant finding of the study is that presence of string cloud parameter leads to the larger horizon compared to the Schwarzschild horizon. As α approaches to unity, the radius of the horizon tends to infinity. Furthermore, it was observed that the effective potential decreases as the string cloud parameter increases. It was noticed that for larger values of the string cloud parameter, the radius of the circular orbit for photons increases. However, it was seen that no stable circular orbit is observed for photons in the presence of string cloud parameter. On the other hand, stable circular orbits were found to exist for the massive particle.

In the third chapter, we have considered static spherically symmetric non-vacuum solution in the presence of electric charge q and Euler-Heisenberg parameter μ. We have calculated radius of horizon and found no difference in the value of outer horizon. However, unlike the RN black hole which possesses two horizons, EH case has one horizon only. Effective potential was evaluated and it was seen that effective potential is not affected by

adding an extra term with new parameter. We have calculated energy and angular momentum as well. There we noticed that reaching minimum circular orbit energy remained positive up to infinite distance. It was shown that there were stable and unstable orbits for particles depending on angular momentum possessing different values.

Bibliography

[1] A. Einstein, Annalen der Physik, 17, 891- 921 (1905).

[2] A. Einstein, Annalen der Physik, 18, 639-641 (1905).

[3] A. Einstein, 15, 176 (1914).

[4] A. Einstein, j-S-B-PREUSS-AKAD-WISS-2, 1030 (1914).

[5] A. Einstein, j-S-B-PREUSS-AKAD-WISS-2, 778 (1915).

[6] K. Schwarzschild, Sitzungsberichte der Königlich Preußischen Akademie der Wissenschaften (Berlin), 1, 189 (1916).

[7] H. Stephani, D. Kramer, M. A. H. MacCallum, C. Hoenselaers and E. Herlt, *Exact Solutions of Einstein's Field Equations*, (Cambridge University Press, 2003).

[8] H. Reissner, Annalen der Physik, 355, 106 (1916).

[9] G. Nordström, Koninklijke Nederlandse Akademie Van Wetenschappen Phys. Sci. B 20, 1238 (1918).

[10] R. P. Kerr, Phys. Rev. Lett. 11, 237 (1963).

[11] E. Newman, E. Couch, K. Chinnapared, A. Exton, A. Prakash and R. Torrence, Math. Phys. 6, 918 (1918).

[12] M. P. Hobson, G. P. Efstathiou and A. N. Lasenby, *General Relativity: An Introduction for Physicist*, (Cambridge University Press, 2006).

[13] V. Frolov and H. Falcke, *The Galactic Black Hole*, (IOP Press, 2003).

[14] R. O. Hansen, Astrophys. J. 8, 170, 557 (1971).

[15] S. Capozziello, A. Foeoli, G. Lambiase, G. Papini and G. Scarpetta, Phys. Lett. A 268, 247 (2000).

[16] N. Dadhich and P. P. Kale, Pramana, 9, 71 (1977).

[17] A. J. Armenti, Il Nuovo Cimento B, 25, 442 (1975).

[18] Z. K. Kurmakaev, Sov. Astron. 18, 110 (1974).

[19] Z. Stuchlik, Bull. Astron. Inst. Czech. 32, 366 (1981).

[20] S. M. Carroll, *Spacetime and Geometry*, (University of Chicago, 2004).

[21] A. Qadir, *Einstein's General Theory of Relativity*, (Cambridge Scholars Publishing, 2020).

[22] B. Schutz, *A First Course in General Relativity*, (Cambridge University Press, 2009).

[23] G. E. Romero and G. S. Vila, *Introduction to Black Hole Astrophysics* (Springer, 2014).

[24] P. S. Joshi, *Gravitational Collapse and Spacetime Singularities* (Cambridge University Press, 2007).

[25] R. Ruffini and J.A. Wheeler, Phys. Today, 24, 30 (1971).

[26] M. Batool and I. Hussain, Int. J. Mod. Phys. D, 26, 1741005 (2017).

[27] P. S. Letelier, Phys. Rev. D, 20, 1294 (1979).

[28] M. Sharif and S. Iftikhar, Adv. High Energy Phys. 2015, 854264 (2015).

[29] J. F. Navarro, C. S. Frenk and S. D. M. White, Astrophy. J. 462, 563 (1996).

[30] L. Samushia and B. Ratra, Astrophys. J. 680, L1 (2008).

[31] N. A. Bahcall, L. M. Lubin and V. Dorman, Astrophys. J. 447 L81 (1995).

[32] L. Sebastiani, S. Vagnozzi and R. Myrzakulov, adv. High Energy Phys. 2017, 3156915 (2017).

[33] B. Wang, E. Abdalla, F. Atrio-Barandela and D. Pavón, Rep. Prog. Phys. 79, 096901 (2016).

[34] H. Weyl, Annalen der Physik, 364, 101-133, (1919).

[35] B. D. Sherwin, J. Dunkley, S. Das et al., Phys. Rev. Lett. 107, 021302 (2011).

[36] A. H. Chamseddine and V. Mukhanov, J. High Energy Phys., 2013, 135 (2013).

[37] E. A. Lim, I. Sawicki and A. Vikman, J. Cosmo. Astropart. Phys. 2010, 12 (2010).

[38] C. Gao, Y. Gong, X. Wang and X. Chen, Phys. Lett. B 702, 107 (2011).

[39] S. Capozziello, J. Matsumoto, S. Nojiri and S. D. Odintsov, Phys. Lett. B 693, 198 (2010).

[40] W. Heisenberg and H. Euler, Z. Phys. 98, 714 (1936).

[41] J. Schwinger, Phys. Rev. 82, 664 (1951).

[42] R. Ruffini, Y.-B. Wu and S.-S. Xue, Phys. Rev. D 88, 085004 (2013).

[43] R. Ruffini, G. Vereshchagin and S.-S. Xue, Phys. Rept. 487, 1 (2010).

[44] K. A. Bronnikov, Phys. Rev. D 63, 044005 (2001).

[45] K. Bronnikov, V. Melnikov, G. Shikin and K. Staniukovich, Annals of Physics 118, 84 (1979).

[46] A. Awad and G. Nashed, J. Cosmo. Astropart. Phys. 2, 46 (2017).

[47] I. Z. Stefanov, S. S. Yazadjiev and M. D. Todorov, Mod. Phys. Lett. A 22, 1217 (2007).

[48] G. G. L. Nashed and S. Nojiri, Phys. Rev. D 104, 044043 (2021).